

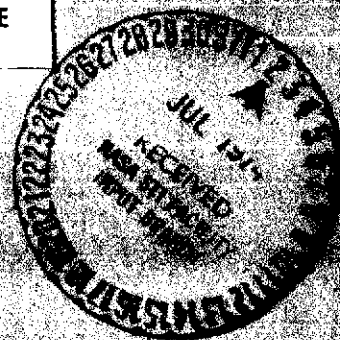
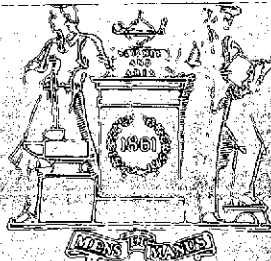
# A STOCHASTIC MODEL OF TURBULENT MIXING WITH CHEMICAL REACTION: NITRIC OXIDE FORMATION IN A PLUG-FLOW BURNER

Richard C. Flagan and John P. Appleton

December 1973

FLUID MECHANICS LABORATORY

Reproduced by  
**NATIONAL TECHNICAL  
INFORMATION SERVICE**  
US Department of Commerce  
Springfield, VA. 22151



(NASA-CR-138628) A STOCHASTIC MODEL OF TURBULENT MIXING WITH CHEMICAL REACTION: NITRIC OXIDE FORMULATION IN A PLUG-FLOW BURNER (Massachusetts Inst. of Tech.)  
64 p Hc \$6.25

CSCI 20D

G3/12

Unclass  
41578

N74-26818

DEPARTMENT OF MECHANICAL ENGINEERING  
MASSACHUSETTS INSTITUTE OF TECHNOLOGY

A STOCHASTIC MODEL OF TURBULENT MIXING WITH CHEMICAL REACTION:  
NITRIC OXIDE FORMATION IN A PLUG-FLOW BURNER

by

Richard C. Flagan and John P. Appleton

ERRATA

Page 18, line 12. Substitute:

...Similarly the probability that mixing will remove a fluid particle in State  $\underline{Z}$  is:

$$n f(\underline{Z}, t) f(\underline{Z}^{(1)}, t) \dots f(\underline{Z}^{(n-1)}, t) d\Omega^{(1)} \dots d\Omega^{(n-1)}$$

If the frequency...

Page 19, line 4. Substitute:

$$- \int_{\Omega}^{(1)} \dots \int_{\Omega}^{(n-1)} 2\omega f(\underline{Z}, t) f(\underline{Z}^{(1)}, t) \dots f(\underline{Z}^{(n-1)}, t) d\Omega^{(1)} \dots d\Omega^{(n-1)} \quad (18)$$

Delete line 5 from Eq. 18.

A STOCHASTIC MODEL OF TURBULENT MIXING WITH CHEMICAL REACTION:  
NITRIC OXIDE FORMATION IN A PLUG-FLOW BURNER

by

Richard C. Flagan and John P. Appleton

Fluid Mechanics Laboratory  
Department of Mechanical Engineering  
Massachusetts Institute of Technology

December 1973

This research was supported in part by the National Aeronautics and Space Administration under Grant: NGR 22-009-378, and by the Environmental Protection Agency under Grant: R-800-729-03-01. This document has been approved for public release and sale; its distribution is unlimited.

A STOCHASTIC MODEL OF TURBULENT MIXING WITH CHEMICAL REACTION:

NITRIC OXIDE FORMATION IN A PLUG-FLOW BURNER

Richard C. Flagan and John P. Appleton  
Department of Mechanical Engineering  
Massachusetts Institute of Technology  
Cambridge, Massachusetts 02139

ABSTRACT

A stochastic model of turbulent mixing has been developed for a reactor in which mixing is represented by  $n$ -body fluid particle interactions ( $n = 2, 3, \dots, 6$ ). The model has been used to justify the assumption (made in previous investigations of the role of turbulent mixing on burner generated thermal nitric oxide and carbon monoxide emissions) that for a simple plug flow reactor, composition nonuniformities can be described by a Gaussian distribution function in the local fuel:air equivalence ratio. Recent extensions of this stochastic model to include the combined effects of turbulent mixing and secondary air entrainment on thermal generation of nitric oxide in gas turbine combustors are discussed. Finally, rate limited upper and lower bounds of the nitric oxide produced by thermal fixation of molecular nitrogen and oxidation of organically bound fuel nitrogen are estimated on the basis of the stochastic model for a plug flow burner; these are compared with experimental measurements obtained using a laboratory burner operated over a wide range of test conditions; good agreement is obtained.

## I. INTRODUCTION

In most practical continuous flow burners, where the fuel and the air enter separately, primary combustion is generally observed to occur within a relatively confined, turbulent, mixing-controlled flame region. The product gases which issue from this primary zone are exceedingly nonuniform both in terms of their species composition and temperature and, in the absence of heat transfer to the surroundings, will only approach the composition of the corresponding adiabatic premixed system after turbulence and diffusive mixing have made the flow more uniform.

There have been several studies carried out recently, notably by Fletcher, Heywood, and their co-workers, e.g. [1-3], which have attempted to examine the role of turbulent mixing within the product gases on burner generated nitric oxide and carbon monoxide formation using the plug-flow reactor concept proposed by Beér and Lee [4]. The important elements of the method developed by these investigators for quantitative modelling of this particular aspect of burner emissions problems are most simply illustrated by the study reported by Pompei and Heywood [3]. These authors carried out an experimental investigation using a relatively simple cylindrical burner in which an atomized spray of kerosene fuel was injected through a nozzle, located on the burner axis, around which combustion air at atmospheric pressure was admitted through swirl vanes. By sampling the mean product gas composition over the cross-section of the burner at several downstream axial positions, it was established that the flow was essentially one-dimensional in the mean over the major portion of the burner length. Therefore, Pompei and Heywood modelled

the flow throughout the burner as a plug-flow by assuming that the fuel was rapidly dispersed throughout the burner cross-section and burned within the primary zone to produce product gases composed of a large number of fluid elements, or eddies, each characterized by a local value of the fuel:air equivalence ratio,  $\phi$ , and each having a scale size much smaller than the burner diameter.

On the basis of the supposition that combustion within the primary zone was entirely mixing-controlled, the major product species within the individual fluid elements were assumed to be present in their equilibrium proportions which, for a fixed pressure, inlet temperature, and given fuel type, were thus uniquely determined by the local value of the fuel:air equivalence ratio and gas temperature. The composition of the product gases at any given downstream cross-section of the burner could therefore be described in terms of a suitably chosen equivalence ratio distribution function,  $f(\phi, t)$ , such that  $f(\phi, t)d\phi$  represented that fraction of the product gases with fuel:air equivalence ratio between  $\phi$  and  $\phi + d\phi$ , with  $t$  being equal to the transit time of the plug-flow between the primary zone and the downstream cross-section. The mean concentration of any major component of the product gases, e.g. CO, O<sub>2</sub>, etc., at a given downstream position in the burner was then expressed in the form:

$$\langle [\text{CO}] \rangle = \int_{\phi} [\text{CO}](T, \phi) f(\phi, t) d\phi \quad (1)$$

where  $T$  is the local temperature--equal to the adiabatic flame temperature for no heat transfer.

It is generally agreed that, for fuels which do not contain organically bound nitrogen, the bulk of burner generated nitric oxide

is formed in the hot product gases via the well known Zel'dovich mechanism. This is an overall endothermic process and, therefore, relatively slow by comparison with the fast hydrocarbon fuel oxidation chemistry. Provided that the local nitric oxide concentration is everywhere less than the corresponding equilibrium concentration, it can be shown that the local rate of formation of nitric oxide by the Zel'dovich mechanism is, to a close approximation, only a function of the local temperature, the local oxygen atom concentration, and the molecular nitrogen concentration. By assuming that the oxygen atom concentration in the product gases was the local equilibrium value and that the local molecular nitrogen mass fraction was essentially unchanged by chemical reactions, it then followed that the local rate of formation of nitric oxide within the fluid elements of the product gases was simply a function of their local temperature and equivalence ratio. Thus, the mean kinetically limited rate of nitric oxide formation at any downstream cross-section of the burner could be expressed in the form:

$$\langle d[\text{NO}]/dt \rangle = \int_{\phi} [\dot{\text{NO}}](T, \phi) f(\phi, t) d\phi \quad (2)$$

and the mean cross-sectional average concentration obtained by integrating over the transit time:

$$\langle [\text{NO}] \rangle = \int_0^t \int_{\phi} [\dot{\text{NO}}](T, \phi) f(\phi, t) d\phi dt \quad (3)$$

In order to apply Eqs. (1) and (3) to calculate the mean concentrations,  $\langle [\text{CO}] \rangle$  and  $\langle [\text{NO}] \rangle$ , a suitable functional form for  $f(\phi, t)$  must be chosen. In the modelling studies referred to above

the form generally adopted has been a Gaussian distribution function:

$$f(\phi, t) = [1/\sqrt{2\pi} \sigma(t)] \exp[-(\phi - \langle \phi \rangle)^2 / 2 \sigma^2(t)] \quad (4)$$

where  $\langle \phi \rangle$  is the mean operating equivalence ratio for the burner and

$$\sigma^2(t) = \langle (\phi - \langle \phi \rangle)^2 \rangle \quad (5)$$

is the variance. Pompei and Heywood determined the variation of  $\sigma^2(t)$  empirically by assuming the Gaussian form for  $f(\phi, t)$  and measuring the mean molecular oxygen concentration along the burner length when it was operated at the overall stoichiometric condition. At this condition,  $\langle [O_2] \rangle$  decreased from easily measurable values at the upstream poorly mixed end of the burner to zero at the downstream end where turbulence and diffusive mixing had rendered the product gases more uniformly mixed. The variation of  $\sigma^2(t)$  was then estimated by matching the measured values of  $\langle [O_2] \rangle$  with those calculated using the expression:

$$\langle [O_2] \rangle = \int_{\phi} [O_2](T, \phi) f(\phi, t) d\phi \quad (6)$$

By arguing that their mixing parameter, defined to be

$$s(t) = \sigma(t) / \langle \phi \rangle, \quad (7)$$

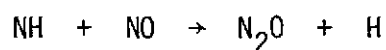
was dependent only on the manner in which the fuel and air were injected into the burner and independent of  $\langle \phi \rangle$ , Pompei and Heywood were able to show that this simple plug-flow mixing model was capable of describing the effects of nonuniformities in the product gases on the burner generated NO and CO concentrations, and that the mixing parameter,  $s(t)$ , could be related, at least empirically, to the



overall burner operating variables such as the fuel atomizing air pressure. The application of this type of model to investigate the effects of changing certain of the operational and design parameters controlling nitric oxide emissions from gas turbine combustors has recently been reviewed by Heywood and Mikus [5].

In this paper we shall address some of the more obvious limitations of this simple mixing model, ultimately directing our attention to the role of turbulent mixing on burner generated nitric oxide formed from organically bound fuel nitrogen for which the simple mixing model is inadequate.

Numerous experimental investigations carried out in both pre-mixed flames [6, 7] and oil fired burners [8-12] have shown that a large fraction of organically bound fuel nitrogen can readily be converted to nitric oxide during combustion. In another paper [13] we examined plausible kinetic models which were shown to be quite successful in explaining the measured nitric oxide yields obtained in premixed flame experiments [6, 7]. On the basis of these models it appears that the yield of nitric oxide by combustion could at least be minimized if the bulk of the fuel could be burned at fuel-rich conditions because, under such conditions, the combustion product species which contain single nitrogen atoms have a greater chance of being removed from the system by reactions of the type:



Indeed, such a view is in keeping with the observations that, whereas, those operational methods which seek to minimize burner generated NO

by reducing peak combustion temperatures (using such techniques as exhaust gas recirculation) are effective for NO formed by thermal fixation of molecular nitrogen (the Zel'dovich mechanism), only variants on the technique of staged combustion (initial burning of the fuel at rich conditions) are effective in reducing the NO formed from fuel nitrogen [12]. With this in mind, it is clearly apparent that in order to construct theoretical models of burner flows which incorporate the combined influence of the fuel nitrogen conversion kinetics and turbulent mixing, it will be essential that:

- (i) they provide an accurate statistical description of the composition nonuniformities in the upstream region of the burner where the bulk of the fuel is contained in kinetically important fuel-rich fluid elements, and
- (ii) allow for the fact that the net rate of removal of NO from the fuel-rich fluid elements is explicitly dependent on the concentrations of product species containing single nitrogen atoms.

To briefly amplify on the first point, it is apparent that even assuming the strictly one-dimensional plug-flow model, the distribution of fuel and air cannot be Gaussian initially but must, more nearly, be bi-modal with one peak corresponding to pure air ( $\phi = 0$ ) and another corresponding to pure fuel ( $\phi = \infty$ ). The question thus arises as to how valid the assumption of a Gaussian distribution in equivalence ratios is as used in the modelling studies referred to previously.

With regard to the second point, the reason why Eq. (2)

may be used to calculate the kinetically limited mean rate of formation of NO is that, according to the Zel'dovich mechanism, the local rate of formation,  $[\dot{\text{NO}}]$ , is explicitly independent of both  $[\text{NO}]$  and  $[\text{N}]$  for  $[\text{NO}] \ll [\text{NO}]_e$ , i.e., it has a zero order dependence on the concentrations of kinetically rate limited species. When  $[\dot{\text{NO}}]$  is not only dependent on  $\phi$  and  $T$  but, also, on the concentrations of rate limited species, which is the case for the conversion kinetics of fuel bound nitrogen [13], the averaging procedure expressed by Eq. (2) is obviously inadequate.

In an attempt to take a more realistic account of the above points, we have employed a stochastic fluid particle interaction model of the turbulent mixing process. The model is developed from the fluid particle collision model of turbulent mixing proposed by Curl [14] to describe mixing in dispersed phase systems and, also, by Evangelista et al. [15, 16] and others [17-19] to describe mixing in both dispersed and continuum systems. As with the simple mixing model, the stochastic model makes no attempt to describe the detailed dynamics of the turbulent flow but, instead, relies on a composition distribution function to describe the nonuniformities in the flow that is itself dependent on an empirically determined mixing intensity parameter. However, although the method is essentially a numerical one, employing a Monte Carlo computational technique, it does allow the shape of the composition distribution function to be determined as it evolves with time, given an initial distribution of fuel and air. At the same time, it allows one to take account of any general chemically rate limited process. Consequently, we have been able to explore the validity of the assumed Gaussian distribution function of the

simple mixing model and, further, have indicated how a more realistic treatment may be made of entrainment or secondary air addition in, for example, gas turbine combustors [5, 20].

Before developing the stochastic model of turbulent mixing, we shall first summarize our experimental measurements of burner generated nitric oxide derived from organically bound fuel nitrogen [11, 21]. Comparisons between the experimental results and model predictions will then follow.

## II. EXPERIMENTAL MEASUREMENTS OF BURNER GENERATED NO FROM FUEL BOUND NITROGEN

Only a brief description of the burner will be given here since it has been described in detail elsewhere [3, 11]. The burner is circular in cross-section, 4 in. internal diameter, and 24 in. long. Combustion air was supplied at atmospheric pressure and admitted at one end through 45° blade-angle swirl vanes. Kerosene doped with small percentages of nitrogen containing additives (pyridine,  $C_5H_5N$ , and pyrrole,  $C_4H_5N$ ), burned at a rate of about 8 lb. hr.<sup>-1</sup> was supplied through a pneumatic atomizer at one end on the burner axis. The air pressure drop across the fuel atomizer was controlled independently of the fuel flow rate, and the air flow through the atomizer only amounted to about 4 percent of the total combustion air. The burner walls were refractory lined to reduce heat losses, and the product gases were sampled with the aid of a fully traversable stainless-steel probe. The composition of the sampled gases was then measured by passing them through an analyzer train. All concentration measurements reported here are cross-sectional averages.

Two series of experiments were carried out in which the total air flow was held fixed at  $125 \text{ lb. hr.}^{-1}$ . In the first series, the fuel flow rate was held constant and the fuel atomizing air pressure was varied to change the fuel-air mixing process within the burner. Low atomizing pressures ( $p \approx 12 \text{ psig}$ ) produced poor initial mixing of the fuel and the air and a highly luminous flame region was observed; higher atomizing pressures ( $p \approx 30 \text{ psig}$ ) produced more intense initial mixing and a blue nonluminous flame region. Figure 1 shows the axial profiles of the nitric oxide concentration obtained at the two extreme atomizing air pressures for the stoichiometric combustion of kerosene doped with 0.51 percent nitrogen by weight in the form of pyridine. Such results are representative of those obtained using different fuel flow rates and different concentrations of fuel nitrogen, i.e., the nitric oxide concentration was observed to rise rapidly to a plateau which, for the largest atomizing pressure and the smallest nitrogen additive concentration (0.25 per by weight), indicated about one hundred percent conversion of the fuel nitrogen to nitric oxide; for lower atomizing pressures, the total conversion of fuel nitrogen was observed to be considerably less. When approximate account was taken of the nitric oxide formed by the Zel'dovich mechanism, this was estimated on the basis of previous measurements [3] performed at the same operating conditions with undoped fuel, the results shown in Figure 1 indicate that about 80 percent of the fuel nitrogen was converted to NO at an atomizing pressure of 29 psig, and at an atomizing pressure of 12 psig the measured NO represents about 50 percent of the fuel nitrogen.

It is apparent, on the basis of the type of results illustrated in Figure 1 that, in addition to the kinetic mechanisms responsible for the conversion of fuel nitrogen to NO, the nature of the nonuniform turbulent mixing processes within the burner must play a very important role in the overall production of NO.

In the second series of experiments, NO concentrations were measured in the exhaust gases, i.e., in the plateau regions of Figure 1, over a wide range of fuel flow rates at different atomizing pressures using both pyridine and pyrrole as additives. These results are plotted in Figures 2a-2c as a function of the operating fuel:air equivalence ratio of the burner; each set of data corresponds to a different proportion of nitrogen in the fuel.

First, it is apparent that, as found in previous premixed flame studies, e.g., Fenimore [6], the percentage conversion of fuel nitrogen to NO is independent of the form in which the nitrogen was added to the fuel. The full lines in Figures 2a-2c represent the NO concentration which would have been found in the exhaust gases for 100 percent conversion of the fuel nitrogen only. The dashed lines represent the sum of 100 percent conversion of the fuel nitrogen plus that, estimated on the basis of previous measurements [3], formed by thermal fixation of  $N_2$ . For well-mixed (high atomizing pressure) lean combustion ( $\phi < 1$ ) and the smallest percentage of fuel nitrogen additive (0.25 percent nitrogen by weight), the measured exhaust NO concentration is seen in Figure 2a to be equal to that estimated on the basis of 100 percent conversion of the fuel nitrogen plus that obtained by thermal fixation. For larger additive concentrations, Figures 2b-2c, the maximum conversion is

somewhat less: about 90 percent for the data in Figure 2b, and 80 percent in Figure 2c. For fuel-rich combustion,  $\phi > 1$ , the percentage conversion of the fuel nitrogen is seen to fall quite drastically. Also, as noted previously, reducing the atomizing pressure at a fixed equivalence ratio has the effect of reducing the NO concentrations in the exhaust.

We have previously reported [11] our attempts to measure the exhaust concentrations of molecules containing CN radicals; our purpose was to establish the possible alternative chemical forms of that fraction of the fuel nitrogen which was not converted to either NO or N<sub>2</sub> when the burner was operated at low fuel atomizing pressures. Briefly, exhaust samples were passed through a gas bubbler containing a basic solution of potassium hydroxide in an attempt to dissolve such molecules as HCN. Titration of this solution with silver nitrate [22] was then followed by the standard confirmatory test for ion CN<sup>-</sup> [23]. Analysis of a sample taken when the burner was operated at the overall stoichiometric condition,  $\phi = 1$ , using fuel doped with 0.51 percent nitrogen as pyridine and an atomizing pressure of 12 psig, indicated an exhaust concentration equivalent to about 30 ppm of HCN. However, it was shown that the efficiency of the system for the dissolution of CN containing species at low concentrations was poor, so this figure could only be considered as a lower limit. We did not pursue this phase of the investigation further because, as will be made apparent in later sections, we now believe that the major portion of the fuel nitrogen in our burner experiments was converted to either NO or N<sub>2</sub>.

### III. MODELS OF TURBULENT MIXING WITH CHEMICAL REACTIONS

#### Corrsin's Model

The mechanics of the interaction between turbulent mixing and chemical reactions has been studied by Corrsin [24-26] for a restricted class of flows, i.e., homogeneous, isotropic, constant density flows. Although Corrsin's model is not applicable to flows of variable density, the results of the simple model will provide a useful test of the stochastic models to be presented in the following section.

Following Corrsin, the flow conservation equation for a chemical species  $i$  with a local concentration  $\Gamma_i$  (mole  $\text{cm}^{-3}$ ) may be written:

$$\partial\Gamma_i/\partial t + \partial(\Gamma_i U_j)/\partial x_j = D \nabla^2 \Gamma_i + R_i(\underline{\Gamma}) \quad (8)$$

where  $x_j$  are the three cartesian position coordinates,

$\underline{\Gamma} = (\Gamma_1, \Gamma_2, \dots, \Gamma_i, \dots)$  is the concentration vector of the chemical species which compose the flow,  $R_i(\underline{\Gamma})$  is the source term representing the production of species  $i$  due to chemical reactions, and  $D$  is the molecular diffusivity which, in Eq. (8) is assumed to be the same for all species.

For a homogeneous flow, i.e., a flow in which the spatial gradients of mean properties are identically zero ( $\partial\langle \quad \rangle/\partial x_j \equiv 0$ ), the equation for the time rate of change of the mean species concentrations is obtained by taking an ensemble average of Eq. (8) over the entire fluid mass:

$$d\langle\Gamma_i\rangle/dt = \langle R_i(\underline{\Gamma}) \rangle \quad (9)$$



The simplest measure of the nonuniformities in composition of such a flow is the concentration variance,  $\langle \gamma_i^2 \rangle$ , where the equation for the time rate of change of the variance is obtained by separating  $\Gamma_i$  in Eq. (8) into its mean and fluctuating components, i.e.,

$$\Gamma_i = \langle \Gamma_i \rangle + \gamma_i ,$$

subtracting Eq. (9) from Eq. (8), multiplying through by  $\gamma_i$ , and again taking an ensemble average; this yields:

$$d\langle \gamma_i^2 \rangle / dt = -2D \langle (\partial \gamma_i / \partial x_j)(\partial \gamma_i / \partial x_j) \rangle + \langle \gamma_i R_i(\underline{\Gamma}) \rangle \quad (10)$$

By further restricting consideration to flows which are isotropic, the three mean square derivatives in Eq. (10) may be characterized in terms of a single local length scale,  $\ell$ , analogous to Taylor's "microscale" of turbulence, to give

$$d\langle \gamma_i^2 \rangle / dt = -(12D/\ell^2) \langle \gamma_i^2 \rangle + \langle \gamma_i R_i(\underline{\Gamma}) \rangle \quad (11)$$

The quantity  $12D/\ell^2$ , which has the units of inverse time, is a measure of the turbulent mixing intensity and will be designated  $\beta(t)$ .

The simple mixing model, referred to in the introduction, used Eq. (9) as the basis for calculating the mean rate of nitric oxide formation by assuming that the local composition of the flow could be represented in terms of a suitably chosen distribution function of equivalence ratios, i.e.,  $f(\phi, t)$ , and that, according to the Zel'dovich mechanism, the chemical source term,  $R_{NO}$ , was only a function of the local equivalence ratio and temperature viz.

$$R_{NO} = [\dot{NO}](T, \phi) \quad (12)$$

The variation of  $f(\phi, t)$ , or more precisely the equivalence ratio variance,  $\sigma^2$ , along the burner was assumed to be governed by an equation similar in form to Eq. (11). However, the assumption that  $\beta$  was independent of the composition was made out of necessity and justified a posteriorie, since it was evident that chemically reactive turbulent flows with heat release could not be regarded as constant density flows.

By considering a single species or group of species whose concentration, denoted by  $\Gamma'_i$ , is unaffected by chemical reactions, for example:

$$\Gamma'_0 = 2[O_2] + [O] + 2[CO_2] + [CO] + [H_2O] + \text{etc.}$$

i.e., any chemical element of the reactive mixture, Eq. (11) may be written in the simplified form:

$$d\langle Y_i'^2 \rangle / dt = -\beta \langle Y_i'^2 \rangle \quad (13)$$

Therefore, if  $\langle Y_i'^2 \rangle$  can be measured along the length of the burner, the local variation of  $\beta$  can be determined from Eq. (13). This is essentially the technique used by Pompei and Heywood except that they assumed that  $\beta$  could be determined from an equation, analogous to Eq. (13), for the variance of the equivalence ratio, viz.

$$d\sigma^2(t) / dt = -\beta \sigma^2(t) \quad (14)$$

By assuming that the equivalence ratio distribution function was Gaussian, see Eq. (4), and that all the major species, specifically the oxygen containing species, were present in their equilibrium proportions at the local temperature  $T$ , they were able to estimate  $\beta$ , using Eq. (14), from measurements of the mean oxygen concentration

obtained along the burner length. It is to be noted that the initial local temperatures in the combustion zone were taken to be the local adiabatic flame temperatures and that these were assumed to decrease linearly along the burner so that the total heat transfer rate from the burner as a whole matched that estimated on the basis of measured outside wall temperatures. Pompei and Heywood thus demonstrated that the square of their mixing parameter,  $s^2(t) = \sigma^2(t)/\langle\phi\rangle^2$ , decreased in an exponential-like manner, in accordance with Eq. (14), with a high value of  $\beta$  in the combustion zone and a lower value thereafter, and furthermore, was only dependent on the fuel atomizing pressure.

#### A Stochastic Mixing Model

A stochastic model of the mixing process may be developed by representing the composition of the fluid at any position in a reactor as an ensemble of fluid particles which are identified in terms of their individual thermodynamic states. The particles are assumed to be sufficiently small with respect to the microscale,  $\lambda$  (see Eq. 11), that the state of each particle may be assumed to be uniform throughout its volume at any instant of time, but the number of particles in a given state may vary with time as a result of pressure changes, chemical reactions, heat transfer, and mixing between particles.

The thermodynamic state of a representative fluid particle is defined in terms of certain of its intensive state properties such as the pressure  $p$ , the specific enthalpy  $h$ , and the species mass fractions  $\underline{Y} = (Y_1, Y_2, \dots, Y_m)$ , where  $m$  is the total number of species contained in the particle. Other representations of the thermodynamic state are clearly possible--see, for example, Galant and Appleton [27].

However, the above representation will be used here and in vector form this may be written:

$$\underline{Z} = (Y, p, h)$$

For a homogeneous, isotropic flow, the state of the ensemble can be described in terms of a time dependent distribution function of thermodynamic states,  $f(\underline{Z}, t)$ . This distribution function is simply the density of representative fluid particles in the  $(m + 2)$ -dimensional thermodynamic state hyperspace of the ensemble, normalized in such a way that

$$\int_{\Omega} f(\underline{Z}, t) d\Omega = 1 : (d\Omega = \prod_{i=1}^{m+2} dZ_i)$$

and thus, if we consider equal mass fluid elements,  $f(\underline{Z}, t) d\Omega$ , is the mass fraction of fluid having a thermodynamic state in the interval  $d\Omega$  centered about  $\underline{Z}$ . The mean value of any property  $g(\underline{Z})$ , for the ensemble is then defined as:

$$\langle g \rangle = \int_{\Omega} g(\underline{Z}) f(\underline{Z}, t) d\Omega$$

In the absence of mixing, temporal changes in  $f(\underline{Z}, t)$  may be formally described by the continuity equation for the concentration of fluid particles in the thermodynamic state space:

$$\partial f(\underline{Z}, t) / \partial t + \sum_{i=1}^{m+2} \partial [f(\underline{Z}, t) R_i(\underline{Z})] / \partial Z_i = 0 \quad (15)$$

The second term may be expanded to explicitly describe the changes in  $f(\underline{Z}, t)$  caused by pressure variations, heat transfer (other than conduction between fluid elements, which will be treated with species mixing), and chemical reactions, respectively, viz.

$$\begin{aligned} \sum_{i=1}^{m+2} \partial[f(\underline{Z}, t) R_i(\underline{Z})] / \partial Z_i &= \partial[f(\underline{Y}, p, h; t) dh/dt] / \partial h \\ &+ \partial[f(\underline{Y}, p, h; t) dp/dt] / \partial p \\ &+ \sum_{i=1}^m \partial[f(\underline{Y}, p, h; t) R_i(\underline{Z})] / \partial Y_i \end{aligned}$$

For an adiabatic (no heat transfer to the reactor walls), constant pressure flow of the type which we shall consider, the first two terms of the above expansion are obviously equal to zero.

The change in the distribution function due to turbulent mixing may be considered by incorporating a mixing term into Eq. (15) to create a master equation of the form:

$$\partial f(\underline{Z}, t) / \partial t + \partial[f(\underline{Z}, t) R_i(\underline{Z})] / \partial Z_i = \{\partial f(\underline{Z}, t) / \partial t\}_{\text{mix}} \quad (16)$$

Any mixing term which conserves the total number of points in the thermodynamic state space, i.e., conserves mass, may, in principle, be applied in Eq. (16). In the following development the mixing term will be evaluated using a model which describes the mixing process as sequence of interactions between randomly chosen groups of  $n$  representative fluid particles which mix completely with one another to form  $n$  new particles having identical thermodynamic states. Between interactions chemical reactions are assumed to proceed within each fluid particle as though it were a closed system. Thus, a class of master equations is defined in which the mixing term is derived in much the same way as the binary collision term ( $n = 2$ ) of the kinetic theory Boltzmann equation in which the particles are assumed to be statistically independent of one another between collisions.

If the ensemble is assumed to be composed of equal mass fluid par-

ticles, a mixing interaction between  $n$  particles with thermodynamic states described by the vectors  $\underline{z}^{(1)}, \underline{z}^{(2)}, \dots, \underline{z}^{(n)}$  will yield  $n$  particles with the same thermodynamic state, viz.

$$z_i = (z_i^{(1)} + z_i^{(2)} + \dots + z_i^{(n)})/n, \quad i = 1, 2, \dots, m + 2 \quad (17)$$

where the pressure,  $p = z_{m+1}$ , is assumed to be constant throughout the flow field. Then the probability that any random interaction between  $n$  particles in states  $\underline{z}^{(1)}, \underline{z}^{(2)}, \dots, \underline{z}^{(n)}$  will produce  $n$  new particles in the particular state  $\underline{z}$  is:

$$\begin{aligned} & n f(\underline{z}^{(1)}, t) f(\underline{z}^{(2)}, t) \dots f(\underline{z}^{(n)}, t) \\ & \times \prod_{i=1}^{m+2} \delta\{(z_i^{(1)} + z_i^{(2)} + \dots + z_i^{(n)})/n - z_i\} d\Omega^{(1)} \dots d\Omega^{(n)} \end{aligned}$$

where the Dirac delta function,  $\delta\{\dots\}$ , is equal to unity when Eq. (17) is satisfied and zero otherwise. Similarly the probability that mixing will remove a fluid particle in state  $\underline{z}$  is:

$$\begin{aligned} & n f(\underline{z}, t) f(\underline{z}^{(1)}, t) \dots f(\underline{z}^{(n-1)}, t) \\ & \times \left[ \prod_{i=1}^{m+2} (1 - \delta\{z_i - (z_i^{(1)} + \dots + z_i^{(n-1)})/(n-1)\}) \right] d\Omega^{(1)} \dots d\Omega^{(n-1)} \end{aligned}$$

If the frequency at which a fluid particle is mixed completely with  $(n-1)$  fluid particles, which may be a function of the local thermodynamic state of the gas, is denoted by  $\omega$ , the net rate of change of  $f(\underline{z}, t)$  due to mixing is obtained by multiplying the probabilities that mixing will increase or decrease  $f(\underline{z}, t)$  by  $\omega$  and then summing over all possible interactions. Thus, Eq. (16) becomes:

$$\begin{aligned}
 & \frac{\partial f(\underline{Z}, t)}{\partial t} + \sum_{i=1}^{m+2} \frac{\partial [f(\underline{Z}, t) R_i(\underline{Z})]}{\partial Z_i} = \\
 & \int_{\Omega} f(\underline{Z}^{(1)}, t) \dots f(\underline{Z}^{(n)}, t) \\
 & \times \left[ \prod_{i=1}^{m+2} \delta \left\{ \frac{Z_i^{(1)} + \dots + Z_i^{(n)}}{n} - Z_i \right\} \right] d\Omega^{(1)} \dots d\Omega^{(n)} \\
 & - \int_{\Omega} f(\underline{Z}, t) f(\underline{Z}^{(1)}, t) \dots f(\underline{Z}^{(n-1)}, t) \\
 & \times \left[ \prod_{i=1}^{m+2} \left( 1 - \delta \left\{ Z_i - \frac{Z_i^{(1)} + \dots + Z_i^{(n-1)}}{n} \right\} \right) \right] d\Omega^{(1)} \dots d\Omega^{(n-1)} \quad (18)
 \end{aligned}$$

For the moment we shall limit our consideration to constant density flows in order to show that the results derived from Eq. (18) are formally quite consistent with Corrsin's, i.e., Eqs. (9) and (11). Assuming constant density,  $\rho$ , the simple transformation

$$\Gamma_i = \rho Y_i / m_i ,$$

where  $m_i$  is the molecular weight of species  $i$ , converts the mass fraction of Eq. (18) to the concentration, e.g., mole  $\text{cm}^{-3}$ , used by Corrsin. Noting the assumption that the molecular diffusivities of all species are the same and that a Lewis number of unity is implicit to our interaction model, the mixing frequency,  $\omega$ , may be assumed to be independent of the fluid particle state. An equation for the time rate of change of the mean thermodynamic state is then obtained by multiplying Eq. (18) by  $\underline{Z}$  and integrating over all  $\underline{Z}$ . This yields

$$d \langle Z_i \rangle / dt - \langle R_i(\underline{Z}) \rangle = 0 \quad (19)$$

which is Corrsin's result.

The equation for the variance of state property  $Z_i$  is obtained by

multiplying Eq. (18) by  $z_i^2 = (Z_i - \langle Z_i \rangle)^2$ , and again integrating over all  $\underline{Z}$ , viz.

$$d\langle z_i^2 \rangle / dt - \langle z_i R_i(\underline{Z}) \rangle = -\omega(n-1)\langle z_i^2 \rangle \quad (20)$$

By comparing Eq. (20) and Eq. (11) we see that they are the same if the mixing frequency,  $\omega(t)$ , is related to  $\beta(t)$  through the expression:

$$\omega(t) = \beta(t)/(n-1) \quad (21)$$

Thus, in the constant density limit the fluid particle interaction model yields the same result as Corrsin's more conventional approach.

If the initial distribution function is known, Eq. (18) may be solved numerically using well known Monte Carlo methods [28] for any general chemical reaction kinetics. We shall assume that, in applying the stochastic mixing model to our burner, the burner may be modelled as a simple plug flow reactor as before. The mixing frequency  $\omega$  is assumed to be equal to  $\beta/(n-1)$  and to be independent of the local gas composition. Thus, we regard  $\omega$  as being empirically determined in the same way as it was when the simple mixing model was applied. The numerical Monte Carlo integration procedure for Eq. (18) is illustrated in Fig. 3 and is briefly described in the following paragraphs.

First, an ensemble of  $N$  equal mass fluid particles is chosen to represent the incoming fluid composition of the burner. Each particle is assumed to be of uniform composition. A fraction of these particles,  $(N_a/N)$ , is taken to represent the flow through the fuel atomizer and to have a composition determined by the equivalence ratio of the atomizer jet ( $\phi_a \gg 1$ ). The remaining particles,  $(N - N_a)$ , represent the pure combustion air,  $\phi = 0$ . Each particle is assigned a number index,  $1 \leq i \leq N$ , and a pseudorandom number generator is then used to generate  $n$  different indices,



$i_1, i_2, \dots, i_n$  ( $i_j \neq i_k$ ), thereby identifying the particles to be involved in the first interaction. They are allowed to mix completely, separate, and react according to the appropriate chemical rate equations. The mixing interactions are computed sequentially, therefore, this first interaction represents a forward step in time equal to

$$\Delta t = 1/\omega(t)N \quad (22)$$

where  $\omega(t)$  is the empirically determined, time dependent mixing frequency. The chemical rate equations are then integrated over the time interval  $\Delta t$ . A new group of  $n$  fluid particles is then chosen at random from the entire ensemble of  $N$  fluid particles to be involved in the next mixing interaction; in this way the calculation proceeds through the burner.

At any time during the mixing process, the mean composition and other mean properties of the fluid in the burner may be evaluated by taking an ensemble average over the  $N$  fluid particles, e.g.

$$\underline{Z} = (1/N) \sum_{i=1}^N \underline{Z}^{(i)} \quad (23)$$

Furthermore, the shape of the evolving distribution function,  $f(\underline{Z}, t)$ , may be determined by plotting the ensemble population as a function of any one of the thermodynamic state variables or any other local property.

Equation (21), i.e.,

$$\omega(t) = \beta(t)/(n-1)$$

guarantees exact correspondence between Corrsin's description of the turbulent mixing process and that based on the stochastic  $n$ -body interaction model for the case of constant density flows. We shall thus

proceed on the assumption that in applying the stochastic model of mixing to the burner flows, the calculations can be performed using the simplest model, i.e.,  $n = 2$ , the binary mixing model, and delay numerical justification until the end of the following section where comparisons between the results will be made using  $n = 2, \dots, 6$ .

#### IV. STOCHASTIC MIXING MODEL RESULTS

##### The Evolution of the Distribution Function

For a burner which admits the fuel and the air separately and which is to be treated as a truly one dimensional plug-flow, the initial distribution function for the fuel and the air will, ideally, be bimodal rather than Gaussian as assumed in the simple mixing model. Nevertheless, the assumption of a Gaussian distribution function did result in good estimates of both the NO and CO emissions [3]. We shall now examine the reasons for the apparent success of the Gaussian distribution function assumption using results obtained from the stochastic mixing model.

The calculations were performed for the case of stoichiometric combustion using the computational procedure outlined in Figure 3. An ensemble of 1000 fluid particles was used to represent the flow. Figure 4 illustrates the shape of the distribution function computed at four downstream positions within the burner as a function of the dimensionless time:

$$\theta = \int_0^t \beta(\tau) d\tau = \zeta(t)/N \quad (24)$$

where  $\zeta(t)$  is the total number of two-particle mixing interactions which have taken place within the ensemble prior to time  $t$ . At early times, when the fluid particles have only mixed an average of once,  $\theta = 1$ , most of the fluid is still contained in either very fuel rich or very lean fluid particles with only a small fraction at or near the stoichiometric condition. Only after each fluid element has mixed three or four times does the distribution function approach a Gaussian distribution, as indicated by the dashed lines in Figure 4.

Now according to the Zel'dovich mechanism, the maximum rate of

formation of nitric oxide occurs only within a narrow range of equivalence ratios about the stoichiometric condition, i.e.,  $0.8 \leq \phi \leq 1.2$ , where the adiabatic flame temperature is highest. The mass fraction of the fluid which, at any time, is responsible for the major portion of the NO production is, therefore,

$$\int_{\phi=0.8}^{1.2} f(\phi, \theta) d\phi$$

In Figure 5 we have compared this fraction, as calculated using the simple mixing model (full line) and the stochastic model (point values), as a function of the dimensionless time  $\theta$ . The agreement between the two is obviously very good even at early time and thus, it is apparent that the reason for the success of the simple mixing model is not that the Gaussian distribution function has the correct overall shape, but that it correctly describes the fraction of the fluid which is contained within the important narrow range of equivalence ratios about the stoichiometric condition.

The simple mixing model also provided reasonable estimates of the mean carbon monoxide concentration within the burner. By assuming that the local CO concentration was the local thermodynamic equilibrium value, it is obvious that only the fraction of fluid which was fuel rich could contain significant CO concentrations. Thus, in Figure 5 we have also compared the mass fraction of the fluid with  $\phi \geq 1.05$ , using both the simple mixing model (broken line) and the stochastic model (point values). For this case it is seen that only for times  $\theta \geq 3$ , do the two predictions agree; for  $\theta < 3$ , the simple model overestimates the fraction of fuel-rich fluid and may thus overestimate the mean CO concentration in the poorly mixed upstream region of the burner. By contrast to the case of NO, the model prediction of the mean CO concentration is dependent on the shape of the distribution

function. To determine the actual extent of this region of discrepancy between the two model predictions requires that we know  $\theta$  as a function of position within the burner.

Now complete combustion can only occur after the fuel and the air have mixed to some degree, and the range of  $\phi$  within which complete combustion is likely to occur is not well defined. However, based upon estimated flammability limits for kerosene [29], we have assumed that complete combustion occurs if  $0.3 \leq \phi \leq 3.0$ , and that no combustion occurs outside these limits. Accordingly, Figure 6 shows the mean oxygen concentration, calculated using the stochastic model for the case of stoichiometric combustion, as a function of the dimensionless mixing time,  $\theta$ . By comparing the values of the mean oxygen concentrations measured as a function of position within the burner [3] with those contained in Figure 6, we were thus able to empirically estimate the variation of  $\theta$  within the burner for different fuel atomizing pressures as illustrated in Figure 7. It can be seen that the variation of  $\theta$  implies that  $\beta(t)$ , see Eq.(24), decreases from a higher value in the upstream region of the burner to a lower one downstream, in accordance with Pompei and Heywood's observations and, furthermore, it is apparent that even at the lowest fuel atomizing pressure,  $\theta$  approaches a value of 3 within the first diameter of the burner length. Thus, the predictions of the mean CO concentrations obtained from the simple mixing model should be reasonable over the major downstream portion of the burner.

In order to incorporate the actual kinetic model for NO production (the Zel'dovich mechanism) into the stochastic model of the burner flow, it would have been necessary to have taken account of the heat losses from the burner. Indeed, the levelling-off of the mean NO concentration with axial distance within the burner, which was observed

experimentally [3], was directly attributable to the fact that the highly temperature sensitive rate of NO formation decreased with axial distance due to the accumulated effect of heat transfer. The approximate iterative method used by Pompei and Heywood to account for heat losses is not so easily incorporated into our stochastic model. For the burner under consideration, the primary mode of heat transfer from the combustion gases to the burner walls was conduction. Although, in principle, this could be modelled by a consideration of the fluid particle interactions with the wall, it would have involved lengthy iterative procedure to match the calculated heat transfer rate to the total heat transfer rate which Pompei and Heywood estimated by a consideration of the natural convection and radiation at the outside wall of the burner, see Section IV reference [3]. Furthermore, without more detailed measurements of the heat transfer rate as a function of axial position, it would be necessary to introduce rather arbitrary and, possibly, questionable assumptions regarding the degree of temperature accommodation which could be achieved between the fluid particles and the wall during interactions. For these reasons and because we have shown that the simple model provides a satisfactory description of the composition nonuniformities over the major portion of the burner length, we have not attempted to incorporate the Zel'dovich mechanism of NO formation into the stochastic model of the burner flow. A more satisfactory test of this aspect of the problem is provided by modelling the NO formation in a more adiabatic burner, i.e., a burner without significant heat transfer effects, such as the gas turbine combustor recently considered by Mikus and Heywood [20]. We shall briefly discuss their results in the following section.

### Gas Turbine Combustor

Nitric oxide formation in conventional gas turbine combustors may be modelled by assuming the primary zone to be a partially stirred reactor to which the simple mixing model, as described earlier, may be applied [1-3,5]. Very little nitric oxide is formed outside the primary zone due to the rapid quenching which occurs with the admission of the secondary air. Mikus and Heywood [5] showed that extensions of this basic model could not adequately describe the NO emissions over the full range of operating conditions of a new combustor design concept presently being developed by NASA [30]. In this design, the NASA modular swirl can combustor, fuel and part of the combustion air (about 10 percent) is introduced through 120 small swirl cans arranged in three concentric rings at the same axial station; most of the remaining combustion air is introduced as flow around the swirl cans.

At very fuel-lean operating conditions, combustion occurs primarily in the small recirculation zones in the wakes of the individual cans. Each reaction zone can thus be treated separately as a partially stirred reactor using the simple mixing model, but including the reverse of the NO formation reactions. By suitably choosing the mixing parameter,  $s$  (see Eq. 7), the NO emissions can be correlated as shown by the lower broken line in Figure 8 [5]. As the overall fuel:air equivalence ratio approaches unity, the individual reaction zones merge so that combustion may then be viewed as occurring throughout the entire volume of the combustion chamber. The correlation illustrated by the upper broken line in Figure 8 was obtained by treating the entire combustor as a partially stirred reactor. It is evident that extrapolations based on these two limiting versions of the simple model do not correlate the NO emissions at intermediate operating conditions.

Mikus and Heywood [20] have recently applied our stochastic mixing model to describe the flow in the NASA swirl can combustor in an attempt to correlate the NO emissions over the full range of operating conditions. The composition of the gases leaving the recirculation zones of the individual swirl cans was assumed to be described by the simple mixing model as applied to a partially stirred reactor. Mixing between this gas and the secondary air which flowed around the swirl cans was then described using the stochastic mixing model. The actual rate of entrainment of the air by the product gases was not treated separately. Instead, the function  $\beta(t)$  was chosen so that the calculated NO emissions gave a best fit to the measured values. Used in this way,  $\beta(t)$  is a combined measure of both the turbulent mixing intensity and the entrainment rate. The full line in Figure 8 illustrates the extremely good correlation which was achieved. A more detailed discussion of these results is contained in the recent paper by Mikus and Heywood [20].

#### Burner Generated Nitric Oxide from Fuel Nitrogen

In a previous paper [13] we proposed a simple kinetic model to describe the yields of nitric oxide measured in the product gases of premixed fuel-rich flames to which a variety of organic fuel nitrogen compounds had been added [6,7]. According to the model the fuel nitrogen is first assumed to be rapidly distributed in its local equilibrium proportions at the adiabatic flame temperature among the species which contain a single nitrogen atom, i.e., NO, N, NH, NH<sub>2</sub>, etc.-- these we designate collectively as RN. The most abundant RN species for local fuel:air equivalence ratios less than about 1.8, is NO. If



the amount of organic nitrogen in the fuel yields a "constrained" equilibrium concentration [27] of RN in excess of the thermodynamic equilibrium value, then its removal will proceed by reactions which ultimately produce  $N_2$ , e.g.



and, accordingly, the rate of removal will be described by a rate equation of the form:

$$d[RN]/dt = -2k(\phi, T)[RN]^2 \quad (25)$$

where the effective rate coefficient is

$$k(\phi, T) = k_1([N]/[RN])_e([NO]/[RN])_e + \dots \\ + k_3([N]/[RN])_e([NH]/[RN])_e \quad (26)$$

and the suffix e denotes equilibrium concentration ratios.

For the simple plug-flow burner under consideration in which the fuel and the air are admitted separately, it is to be anticipated that most of the fuel will first be burnt in fuel-rich fluid elements. Thus, in applying the stochastic model of the mixing process to the burner, we see that the fractional reduction in the concentration of RN in a fuel-rich fluid particle is given by an expression obtained by integrating Eq. 25 with respect to time, viz.

$$[RN]/[RN]_{\Delta t=0} = 1/(1 + \Delta t/\tau) \quad (27)$$

where  $\Delta t$  is the time measured between interactions and the characteristic reaction time,  $\tau$ , is defined to be:

$$\tau = 1/(2k(\phi,T)[RN]_{\Delta t=0}) \quad (28)$$

Figure 9 illustrates the variation of the effective rate coefficient,  $2k(\phi,T)$ , as a function of the fuel:air equivalence ratio for the adiabatic combustion of kerosene fuel at atmospheric pressure. The rate coefficients:  $k_1, k_2$ , etc., which are contained within the definition of  $k(\phi,T)$  were evaluated using the expressions given in reference [13].

Figure 10 illustrates the variation the NO concentration, calculated on the basis of complete thermochemical equilibrium, as a function of fuel:air equivalence ratio--also for the case of adiabatic kerosene fuel combustion. The broken line illustrates the nitric oxide concentration in the product gases which could be formed if the fuel nitrogen (0.51 percent by weight as N in the fuel) were converted to the species RN on the basis of the constrained equilibrium assumption. According to the kinetic model, the rich fluid particles which fall within the cross-hatched area of Figure 10 will lose fuel nitrogen at a rate given by Eq. 25. However, after mixing with air or more fuel-lean fluid, the composition will change and the representative particles may then be located at positions to the left of the cross-hatched region. In this region the NO concentration will be less than the corresponding equilibrium concentration (indicated by the full line) and thus the rate of removal of the RN species will be exceeded by the formation of NO via the Zel'dovich mechanism. As we have indicated previously, significant rates of NO formation by thermal fixation only

occur for fluid with fuel:air equivalence ratios between about 0.8 and 1.2. At lower equivalence ratios the rate of formation is very slow due to the low local temperatures. For that portion of the fluid which, by further mixing, is characterized by fuel:air equivalence ratios less than about 0.5, the local NO concentrations may again be far in excess of the local equilibrium values. However, due to the exceedingly low concentrations of all of the RN species other than NO at such low equivalence ratios, further removal of NO via reactions (1) - (3) will be virtually halted on time scales comparable with the flow transit times through the burner.

With this qualitative description of the mixing process in mind we see that, to a first approximation, the rate of formation (destruction) of NO within the burner may be modelled by first assuming that the NO derived from the fuel nitrogen is formed at a rate independent of the amount formed by thermal fixation. Thus, the fuel derived NO may be calculated using the stochastic model of the mixing process by applying Eq. 26 to describe the rate of RN removal within each fluid particle between interactions. In carrying out this calculation, no account need be taken of the effects of accumulated heat transfer from the burner which gives rise to an exhaust gas temperature drop of about 200°-300° K [3]. This assumption is justified by observing that the rate of NO removal as described by Eq. 25 is relatively insensitive to such small temperature variations--certainly much less so than is the rate of NO formation by the Zel'dovich mechanism. The total nitric oxide concentrations within the burner may then be obtained by adding to these results the additional NO which is formed by thermal fixation--the latter being estimated on the basis of Pompei and Heywood's simple mixing model calculations which include the effects of heat transfer.

Obviously, this combined model for calculating the total NO formation will provide an upper bound to the NO concentrations within the burner. The reason for this is that the model takes no account of the fact that some fraction of the thermally derived NO, which is formed in fluid with a near stoichiometric composition, will be mixed into fuel-rich fluid and may, therefore, be removed by reactions (1) - (3) at a rate described by Eq. 25. The magnitude of this error may be examined by considering a fuel-rich fluid particle which has a residence time  $\Delta t$  between mixing interactions and an initial single nitrogen species concentration:  $[RN] = [RN]_f + [RN]_t$ , where  $[RN]_f$  refers to the concentration derived from the fuel nitrogen and  $[RN]_t$  refers to the concentration formed by prior thermal fixation. According to the combined model, the RN concentration after time  $\Delta t$  will be

$$[RN]_{\Delta t}' = [RN]_t + [RN]_f / (1 + 2\Delta tk(\phi, T)[RN]_f) \quad (29)$$

whereas, in reality, the removal reactions should also affect the NO formed by thermal fixation, viz.

$$[RN]_{\Delta t} = ([RN]_t + [RN]_f) / (1 + 2\Delta tk(\phi, T)([RN]_t + [RN]_f)) \quad (30)$$

In the limit,  $\Delta t/\tau = 2\Delta tk(\phi, T)[RN] \ll 1$ , the two results are obviously identical. However, for  $\Delta t/\tau \gg 1$ , we see that

$$[RN]_{\Delta t}' = [RN]_t + [RN]_{\Delta t} \quad (31)$$

i.e., the difference between  $[RN]_{\Delta t}'$  and  $[RN]_{\Delta t}$  may amount to as much as  $[RN]_t$ . Thus, we are in a position to calculate both an upper bound to the NO emissions, i.e., the result of the combined model, and a lower

bound--obtained by neglecting the contribution due to thermal fixation.

Calculations were carried out with the stochastic mixing model and the fuel nitrogen conversion kinetics model, as described above, for the burner operating conditions that corresponded to the experiments reported in Section II. Values of the mixing intensity,  $\beta$ , were deduced by matching the calculated mean axial oxygen concentration profiles with those measured by Pompei and Heywood. Satisfactory fits to the data at each atomizing pressure were obtained by choosing an initial value of the mixing intensity,  $\beta_1$ , which remained constant in the upstream portion of the burner for a mean transit time  $t_\beta$ . Thereafter, the mixing intensity assumed a lower value  $\beta_2$ , which appeared to be independent of the atomizing pressure. These empirically determined values of  $\beta_1$ ,  $\beta_2$ , and  $t_\beta$ , are given in Table I as a function of the fuel inlet air atomizing pressure.

Axial profiles of the calculated mean NO concentrations for the case of overall stoichiometric combustion (0.51 percent nitrogen by weight in the fuel) at the two extremes of the fuel atomizing pressure are compared with the experimental measurements in Figure 11. The full lines, estimated on the basis of the stochastic model, illustrate the contribution of the fuel nitrogen alone; the broken lines add to this the NO formed by thermal fixation and were estimated using the simple mixing model. For the well mixed case ( $p = 29$  psig) the broken line closely approximates to the measured profile. The reason for this agreement is that at high fuel atomizing pressures the residence time of the fuel in the rich regions of the flow is curtailed by rapid mixing, thereby, minimizing the effect of reactions (1) to (3) which reduce the fuel nitrogen to  $N_2$ . By contrast, it can be seen that at the lowest atomizing pressure consideration of only the fuel nitrogen

kinetics, as shown by the full line in Figure 11, yields good agreement with the measured NO concentration in the exhaust. The reason for this stems from the fact that mixing takes place sufficiently slowly at the lowest atomizing pressure that a large proportion of the RN species (about 40% of the original fuel nitrogen) can be converted to  $N_2$  in the fuel-rich fluid. Clearly, this case approximates the asymptotic limit for which the residence times of representative fuel-rich fluid particles are much longer than the characteristic chemical conversion times.

One feature of the calculated axial NO profile which is not reflected in the measurements is the maximum which occurs at about one diameter downstream from the fuel inlet nozzle. This discrepancy suggests that the one dimensional plug-flow model does not accurately represent the position-time history of the flow in the upstream region of the burner. We can only speculate that recirculation, which is necessary to stabilize combustion in the actual burner, is responsible. Certainly, a recirculation zone would have the effect of smoothing out the peak in the measured cross-sectional average NO concentration.

Figures 12(a) - 12(d) show comparisons between the calculated and measured mean NO concentrations in the burner exhaust for the full range of fuel atomizing pressures as a function of the overall fuel:air equivalence ratio. For the case of well mixed combustion ( $p = 29$  psi) the prediction of the combined model (broken line in Figure 12(a)) is clearly in good agreement with the measurements over a large proportion of the range of equivalence ratios investigated. Again, this indicates that the intense mixing at this condition does not allow sufficient time for the fuel nitrogen to be reduced to  $N_2$  within the fuel-rich fluid

elements. For the lowest atomizing pressure ( $p = 12$  psig) it appears that the contribution of thermal fixation to the NO exhaust emissions is small at all equivalence ratios since the measurements fall closely about the stochastic mixing model prediction which only accounts for the fuel nitrogen conversion kinetics. By including the comparisons which have been made in Figures 12(b) - 12(c) for the two intermediate fuel atomizing pressures, we recognize an obvious trend in the functional dependence of the exhaust NO concentrations on both the overall equivalence ratio and the fuel atomizing pressure, namely: the equivalence ratio at which the combined model ceases to correlate the measured NO emissions decreases as the fuel atomizing is lowered. Even at the highest atomizing pressure, Figure 12(a), the two data points at equivalence ratios greater than 1.3 are seen to lie closer to the lower bound estimate. In order to calculate the exhaust NO emissions which fall midway between the upper and lower bound estimates it would be necessary to include thermal fixation in the stochastic model and, although this is easily incorporated, it would require that an accurate account of the heat losses from the burner be included.

Figures 13(a) - 13(b) and 14(a) - 14(b) show comparisons between our upper and lower bound model predictions and the measurements of the exhaust NO concentrations as a function of equivalence ratio for fuel nitrogen additive concentrations of 0.25 and 1.06 percent by weight nitrogen, respectively. The same general trends are observed for the well mixed and poorly mixed conditions as were described above. However, it is now apparent that the lower bound prediction overestimates the NO yield by about 20 percent for the case of the highest fuel nitrogen additive concentration and the lowest atomizing pressure. We can only

speculate that the reason for this stems from the inadequacy of our simplified model of the fuel nitrogen conversion kinetics. The assumption that the fuel nitrogen is initially distributed amongst all the possible single nitrogen species, including N and NO, is probably suspect for the very fuel-rich fluid elements--a point which we discussed in our previous paper [13]. Until a better and more exact understanding of the fuel nitrogen conversion kinetics has been developed, we cannot profitably pursue this application of the burner mixing model further.

Approximate numerical justification for the validity of the relationship

$$\omega(t) = \beta(t)/(n-1)$$

for variable density flows with finite rate chemistry and heat release is provided by the results shown in Figure 15a and 15b. For each mixing model, i.e.,  $n = 2, 3, 4, 5$  and  $6$ , values of  $\beta_1$ ,  $t_\beta$  and  $\beta_2$  were chosen so that the computed values of the mean molecular oxygen concentration were closely matched to the measured values as a function of axial position within the burner. By comparing these values, see legend to Figure 15, it can be seen that in no case do the values differ by more than 12 percent; this difference is probably within the statistical uncertainty of the calculations caused by the finite number of particles in the ensemble ( $N = 500$  for all results shown in Figure 15).

The close agreement between the mean NO concentration profiles shown in Figure 15b implies that each model is capable of correctly representing the mixing-composition-time history of the flow as a whole. In view of this it seems that the stochastic nature of the turbulent mixing process is the central most important aspect of the mixing models and that the details of the interaction, i.e., the



number of fluid particles involved or the equal mass assumption, is relatively unimportant. Indeed, it is likely that other stochastic model representations of the mixing term in the master equation, Eq. 16, could be made to work equally well. However, from a practical point of view it appears that the simple binary mixing model is justified in describing the type of burner flow considered here.

## V. CONCLUSIONS

In this investigation we have developed a stochastic model of turbulent mixing for a plug flow reactor in which mixing is represented by random fluid particle interactions. The model was developed for the purpose of investigating the role of composition nonuniformities on burner emission characteristics. As with previous mixing models such as the partially stirred or plug flow reactor concepts, no attempt is made to describe the detailed dynamics of the turbulent flow. Instead, the composition of the flow is assumed to be described in terms of a distribution function of thermodynamic states which evolves with time by the action of general rate limited chemical processes and mixing. The mixing process is characterized in terms of an empirically determined "mixing frequency" which has been shown to bear a direct relationship to the more familiar mixing rate intensity as used, for example, by Corrsin. The model thus represents the flow as an ensemble of perfectly stirred reactors, each characterized by its own thermodynamic state, which are created and destroyed by fluid particle mixing. Between interactions, chemical reactions are assumed to proceed at the finite rates dictated by appropriate kinetic models as though each reactor (fluid particle) were a closed system.

On the basis of this stochastic mixing model we have shown that the simple plug flow mixing model (developed by previous authors to investigate the role of turbulent mixing on burner generated thermal NO and CO), which assumes that the composition nonuniformities can be described by a Gaussian distribution function in the local fuel:air equivalence ratio, is justified.

The stochastic model has also been extended to include the combined effects of turbulent mixing and secondary air entrainment on thermally generated NO in gas turbine combustors. The model enabled measured NO emissions of a new modular combustor design to be correlated over a wide range of fuel:air ratios in terms of a single empirically determined mixing/entrainment rate parameter.

Finally, we have used the stochastic mixing model to predict rate limited upper and lower bound estimates on the yield of burner generated NO formed both by thermal fixation and from organically bound fuel nitrogen. The resulting comparison which we were able to make between the model predictions and the measured NO yields served to illustrate that the stochastic mixing model can be used to relate burner emissions to such operating variables as fuel atomizing pressure, overall equivalence ratio, and fuel nitrogen additive concentration. Furthermore, we conclude that quantitative agreement of the model predictions and the measurements in this latter application was only limited by insufficient information on the local rate of heat loss from the burner and by possible inadequacies in the kinetic model of fuel nitrogen oxidation and reduction.

### ACKNOWLEDGMENT

This work was supported in part by the National Aeronautics and Space Administration under Grant NGR 22-009-378 and by the Environmental Protection Agency under Grant R-800-729-03-01. Part of the work was presented at the A.I.Ch.E. 66th Annual Meeting under the title: Nitric Oxide Formation from Fuel Bound Nitrogen in an Oil Fired Burner.

We would like to express our thanks to several of our colleagues for helpful discussions, notably Professor D. P. Hoult, who suggested extending our investigation of the stochastic mixing model beyond the two-particle limit.

One of us (R.C.F.) wishes to acknowledge partial financial support from M.I.T. for a Sloan Research Traineeship.

TABLE I

Mixing Intensity

p (psig)	$\beta_1(\text{sec}^{-1})$	$t_\beta(\text{sec})$	$\beta_2(\text{sec}^{-1})$
29	400	.0205	60
20	300	.021	60
17.5	252	.0216	60
15	200	.023	60
12	112	.025	60

VI. REFERENCES

1. Fletcher, R. S., and Heywood, J. B., "A Model for Nitric Oxide Emissions from Aircraft Gas Turbine Engines," AIAA Paper 71-123, presented at AIAA 9th Aerospace Sciences Meeting, New York, January 1971.
2. Mikus, T., and Heywood, J. B., Combustion Sci. & Tech. 4, 149-158 (1971).
3. Pompei, F., and Heywood, J. B., Comb. & Flame 19, 407-418 (1972).
4. Beér, J. M., and Lee, K. B., Tenth Symposium (International) on Combustion, The Combustion Institute, Pittsburgh, Pa. (1965) pp. 1187-1202.
5. Heywood, J. B., and Mikus, T., "Parameters Controlling Nitric Oxide Emissions from Gas Turbine Combustors," paper presented at the AGARD Propulsion and Energetics Panel, 41st Meeting on Atmospheric Pollution by Aircraft Engines, London, England, 9-13 April 1973.
6. Fenimore, C. P., Comb. & Flame 19, 289 (1972).
7. Johnson, C. T., "The Conversion of Fuel Bound Nitrogen to Nitric Oxide in Low Volatile Pulverized Coal Flames," S.B. Thesis, Dept. of Chemical Engineering, M.I.T., Cambridge, Ma., 1973.
8. Bartok, W., Crawford, A. R., and Skopp, A., Chem. Eng. Prog. 64, 64 (1971).
9. Bartok, W., Engleman, V. S., Goldstein, R., and del Valle, E. G., "Basic Kinetic Studies and Modeling of Nitrogen Oxide Formation in Combustion Processes," presented at Symposium on Combustion Processes and Air Pollution Control, A.I.Ch.E. 70th Annual Meeting, Atlantic City, August 29, 1971.
10. Martin, G. B., and Berkau, E. E., "An Investigation of the Conversion of Various Fuel Nitrogen Compounds to Nitrogen Oxides in Oil Combustion," presented at Symposium on Combustion Processes and Air Pollution Control, A.I.Ch.E. 70th Annual Meeting, Atlantic City, August 30, 1971.
11. Appleton, J. P., and Heywood, J. B., Fourteenth Symposium (International) on Combustion, The Combustion Institute, Pittsburgh, Pa. (1972) pp. 777-786.
12. Turner, D. W., and Siegmund, C. W., "Staged Combustion and Flue Gas Recycle: Potential for Minimizing  $\text{NO}_x$  from Fuel Oil Combustion," presented at American Flame Research Committee Flame Days, Chicago, Illinois, September 6-7, 1972.

13. Flagan, R. C., Galant, S., and Appleton, J. P., "Rate Constrained Partial Equilibrium Models for the Formation of Nitric Oxide from Organic Fuel Nitrogen," M.I.T. Fluid Mechanics Lab. Report 73-7, July 1973. Accepted for publication in Comb. and Flame.
14. Curl, R. L., A.I.Ch.E. J. 9, 175 (1963).
15. Evangelista, J. J., Katz, S., and Skinner, R., A.I.Ch.E. J. 15, 843 (1969).
16. Evangelista, J. J., Skinner, R., and Katz, S., Twelfth Symposium (International) on Combustion, The Combustion Institute, Pittsburgh, Pa. (1968).
17. Spielman, L. A., and Levenspiel, O., Chem. Eng. Sci. 20, 247 (1965).
18. Shain, S. A., A.I.Ch.E. J. 12, 806 (1966).
19. Rao, D. P., and Dunn, I. J., Chem. Eng. Sci. 25, 1275 (1970).
20. Mikus, T., and Heywood, J. B., "Nitric Oxide Formation in the NASA Swirl-Can Combustor, to be presented at the Winter Annual Meeting of the A.S.M.E., Detroit, Mich., Nov. 11-15, 1973.
21. Flagan, R. C., "The Formation of Nitric Oxide from Organic Fuel Nitrogen Contained in Fossil Fuels," Ph.D. Thesis, Mechanical Engineering Department, M.I.T., Cambridge, Ma., May 1973
22. Jacobs, M. B., The Analytical Toxicology of Industrial Inorganic Poison, Interscience, 1967, p. 433.
23. Noyes, A. A., and Swift, E. H., Qualitative Chemical Analysis of Inorganic Substances, Macmillan, 1942, p. 329.
24. Corrsin, S., A.I.Ch.E. J. 3, 329 (1957).
25. Corrsin, S., Phys. Fluids 1, 42 (1958).
26. Corrsin, S., A.I.Ch.E. J. 10, 870 (1964).
27. Galant, S., and Appleton, J. P., "The Rate-Controlled Method of Constrained Equilibrium Applied to Chemically Reactive Open Systems," M.I.T. Fluid Mechanics Lab. Report 73-6, July 1973.
28. Hammersley, J. M., and Handscomb, D. C., Monte Carlo Methods, Methuen and Co., Ltd., London (1964).
29. -- "Basic Considerations in the Combustion of Hydrocarbon Fuels with Air," NACA Report No. 1300, Propulsion Chemistry Div., Lewis Flight Lab. 1951.
30. Niedzwiecki, R. W., and Jones, R. E., "Pollution Measurements of a Swirl Can Combustor, A.I.A.A. Paper No. 72-1201, AIAA/SAE 8th Joint Propulsion Specialists Conference, New Orleans, 29 December 1972.

FIGURE CAPTIONS

- Fig. 1 Axial variation of NO concentration (ppm, wet basis) during combustion of kerosene with 0.51 percent nitrogen by weight added as pyridine.
- Fig. 2 Exhaust NO concentrations for combustion of nitrogen containing fuels. Filled symbols: pyridine additive; Open symbols: pyrrole additive.  $\circ$ , p = 29 psig;  $\square$ , p = 20 psig;  $\diamond$ , p = 17.5 psig;  $\triangle$ , p = 12 psig.
- Fig. 3 Computer code flow diagram for stochastic mixing model. Note:  $\underline{z}^{(i)} = (z_1^{(i)}, z_2^{(i)}, \dots, z_k^{(i)}, \dots)$ , where  $z_k^{(i)}$  is  $k^{\text{th}}$  intensive state property of  $i^{\text{th}}$  fluid particle.
- Fig. 4 Distribution function  $f(\phi)$  as a function of dimensionless time  $\theta$ . Broken line - Gaussian distribution function.
- Fig. 5 Mass fraction of fluid within specified ranges of equivalence ratio plotted as a function of the dimensionless time  $\theta$ . Points represent the stochastic mixing model evaluation and the lines represent the Gaussian distribution function evaluation.
- Fig. 6 Variation of the oxygen concentration with the dimensionless time  $\theta$  calculated for stoichiometric combustion using the stochastic mixing model.
- Fig. 7 Variation of  $\theta$  with axial distance along burner evaluated using oxygen concentration measurements of Pompei and Heywood [3].
- Fig. 8 Comparison of measured and calculated nitric oxide emissions from the NASA swirl can combustor [20] at an operating pressure of 5 to 6 atm. Broken lines: simple mixing model calculations; full line: stochastic mixing model calculation.
- Fig. 9 Variation of effective rate coefficient for RN removal reactions as a function of fuel:air equivalence ratio for adiabatic combustion of kerosene.
- Fig. 10 Equilibrium nitric oxide concentration as a function of equivalence ratio for adiabatic combustion of kerosene.
- Fig. 11 Comparison of measured and calculated axial nitric oxide concentration profiles for combustion of kerosene with 0.51 percent nitrogen added as pyridine. Full lines: fuel nitrogen contribution alone; broken lines: combined model predictions.

- Fig. 12 Comparison of measured and calculated NO emissions from combustion of kerosene with 0.51 percent nitrogen added as pyridine, ●, and pyrrole, ○. Full lines: fuel nitrogen contribution by stochastic model; broken lines: combined model predictions.
- Fig. 13 Comparison of measured and calculated NO emissions from combustion of kerosene with 0.25 percent nitrogen added as pyridine, ●, and pyrrole, ○. Full lines: fuel nitrogen contribution by stochastic model; broken lines: combined model prediction.
- Fig. 14 Comparison of measured and calculated NO emissions from combustion of kerosene with 1.06 percent nitrogen added as pyridine, ●, and pyrrole, ○. Full lines: fuel nitrogen contribution by stochastic model; broken lines: combined model prediction.
- Fig. 15 Comparison of stochastic model calculations for  $n = 2, 3, \dots, 6$ .  
(A) ● Measured oxygen concentrations.  
Calculated oxygen concentrations:  
○:  $n = 2, \beta_1 = 200 \text{ sec}^{-1}, \tau = 0.024 \text{ sec}, \beta_2 = 60 \text{ sec}^{-1}$ ;  
□:  $n = 3, \beta_1 = 200 \text{ sec}^{-1}, \tau = .021 \text{ sec}, \beta_2 = 60 \text{ sec}^{-1}$ ;  
◇:  $n = 4, \beta_1 = 200 \text{ sec}^{-1}, \tau = .021 \text{ sec}, \beta_2 = 60 \text{ sec}^{-1}$ ;  
△:  $n = 5, \beta_1 = 200 \text{ sec}^{-1}, \tau = .021 \text{ sec}, \beta_2 = 60 \text{ sec}^{-1}$ ;  
▽:  $n = 6, \beta_1 = 175 \text{ sec}^{-1}, \tau = .023 \text{ sec}, \beta_2 = 52.5 \text{ sec}^{-1}$ .  
(B) Calculated fuel nitrogen concentrations: [RN], open symbols; [NO], filled symbols.



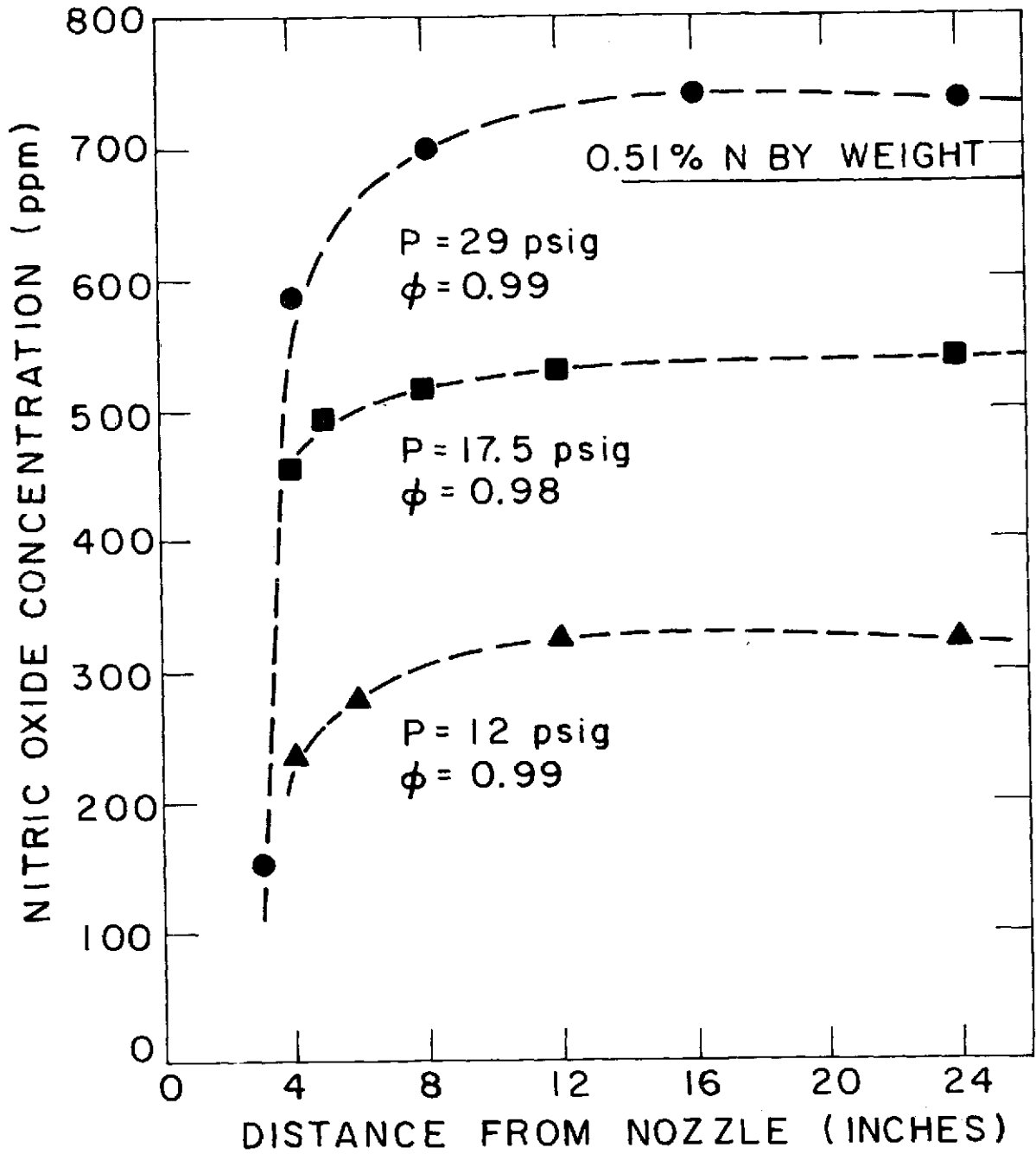


FIGURE 1

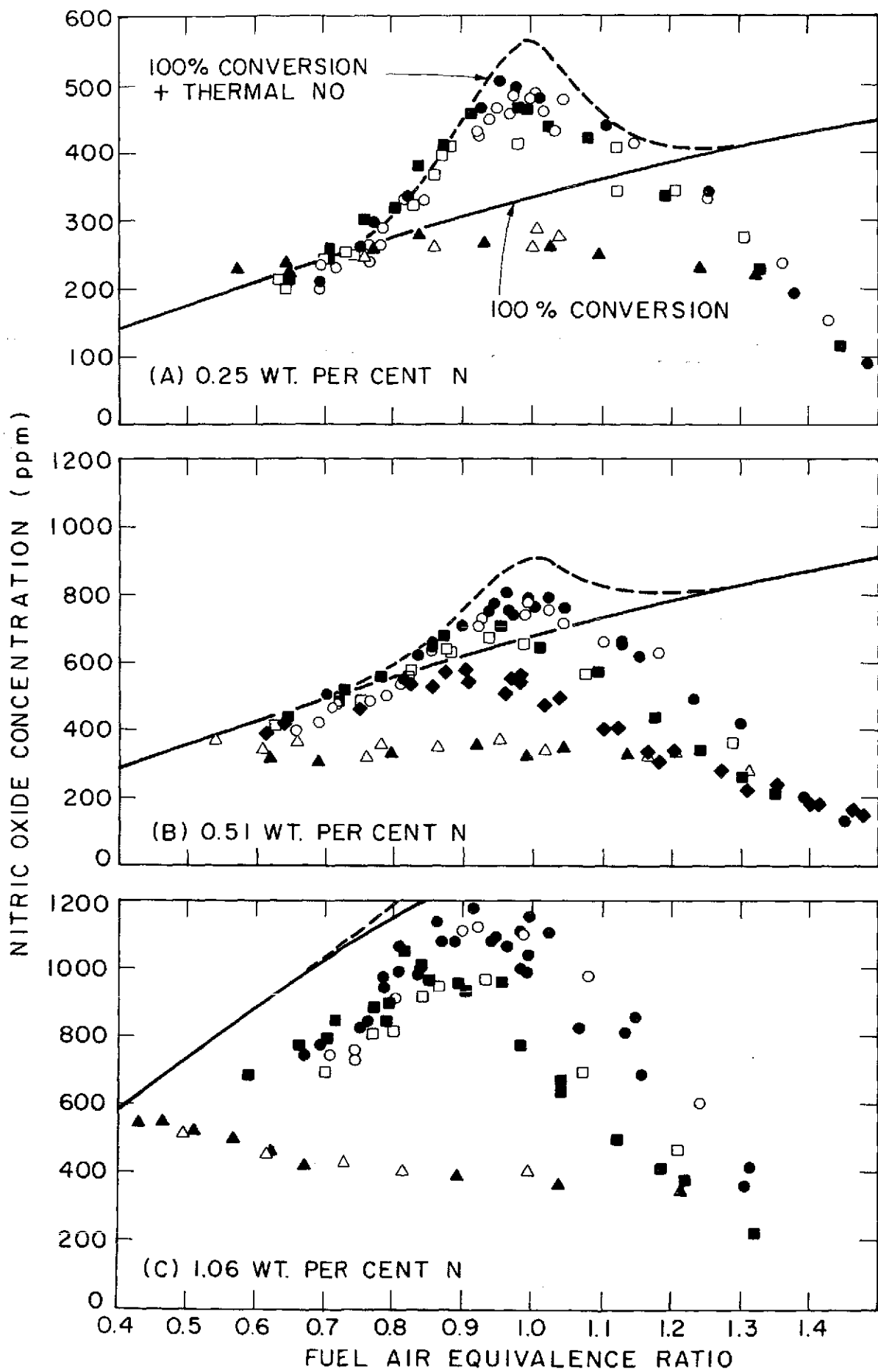


FIGURE 2

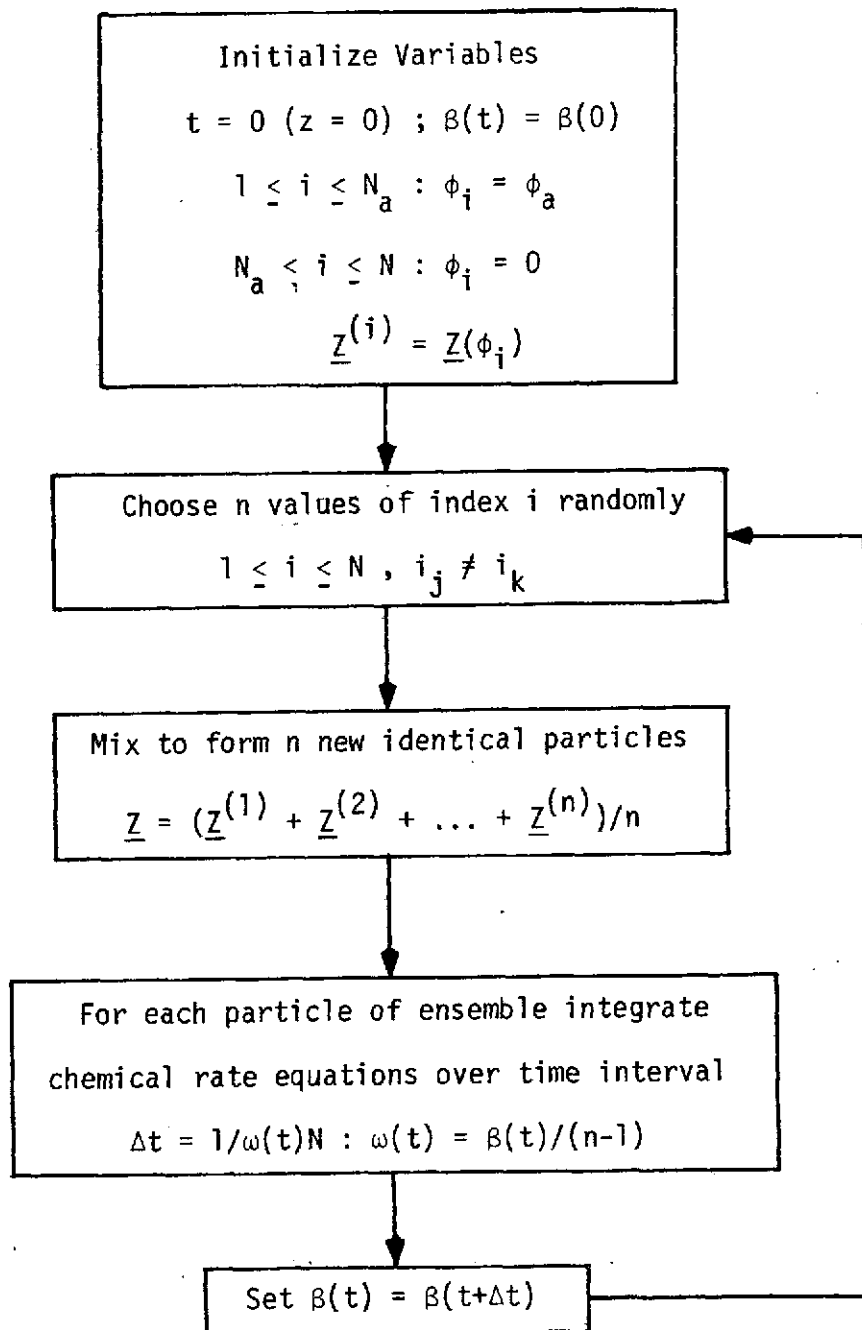


Figure 3. Computer Code Flow Diagram for Stochastic Mixing Model

Note:  $Z_1^{(i)} = (Z_2^{(i)}, Z^{(i)}, \dots, Z_k^{(i)}, \dots)$ , where  $Z_k^{(i)}$  is the  $k^{\text{th}}$  intensive state property of the  $i^{\text{th}}$  fluid particle.

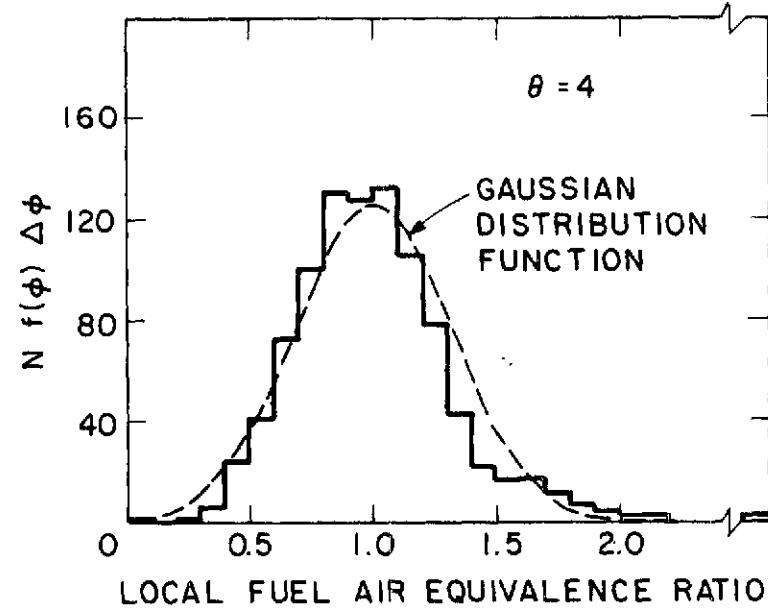
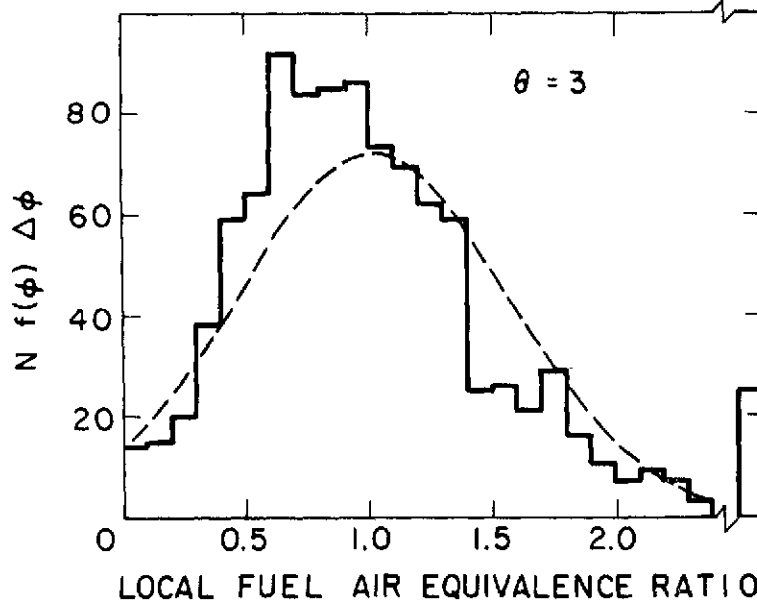
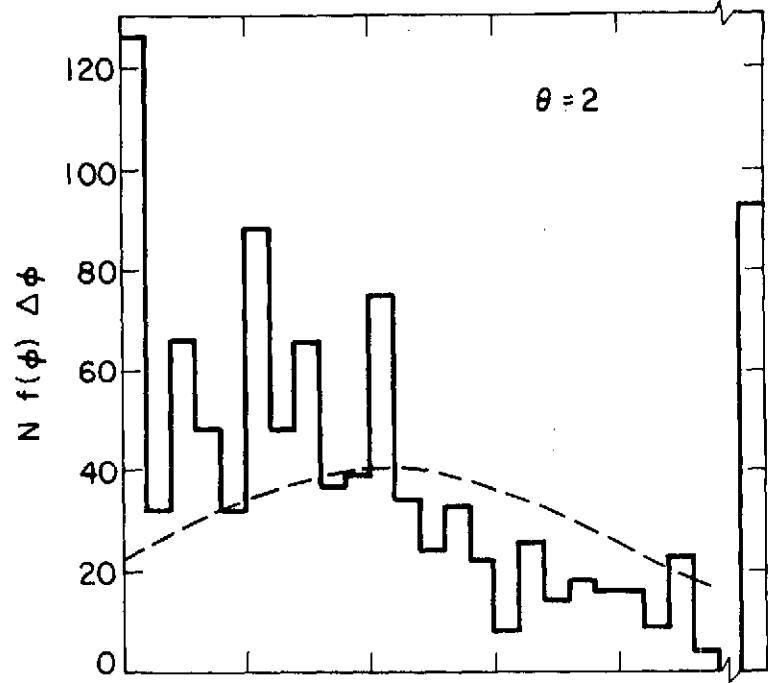
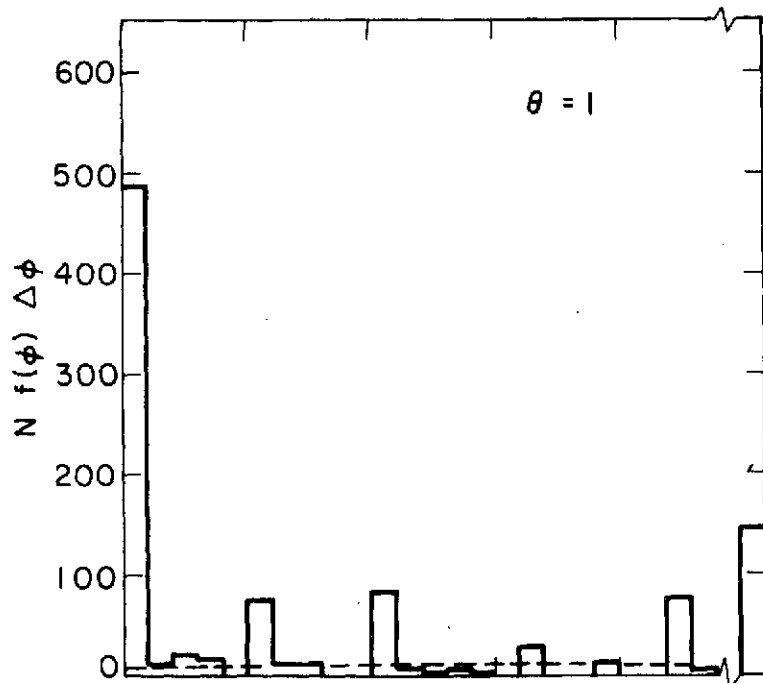


FIGURE 4

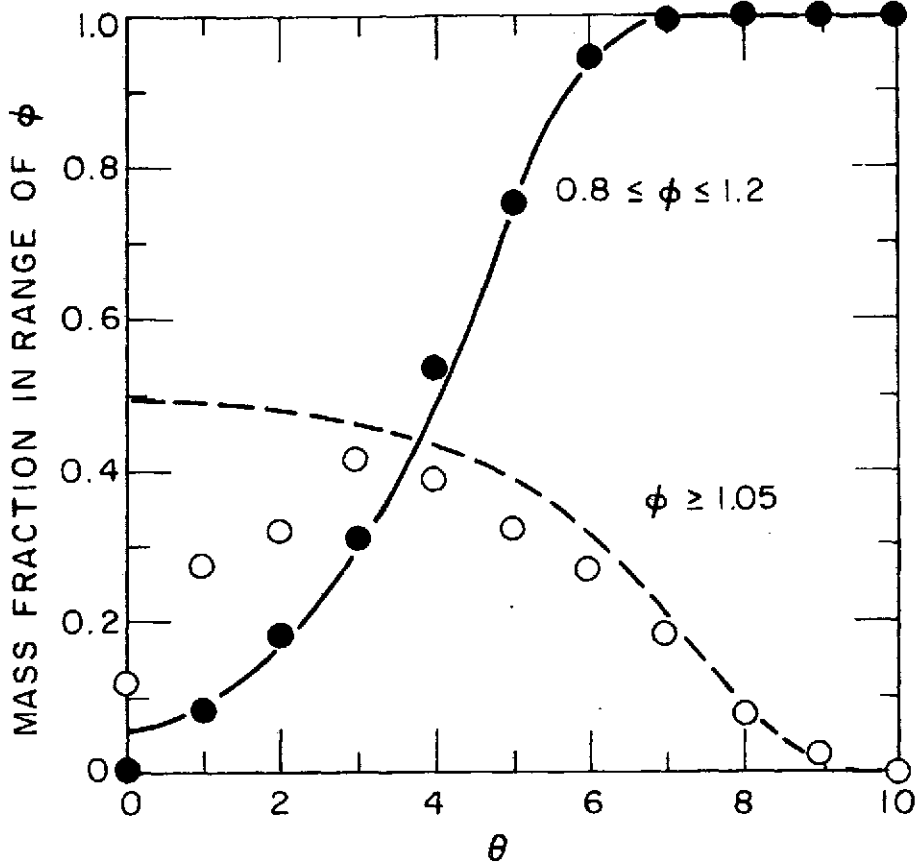


FIGURE 5

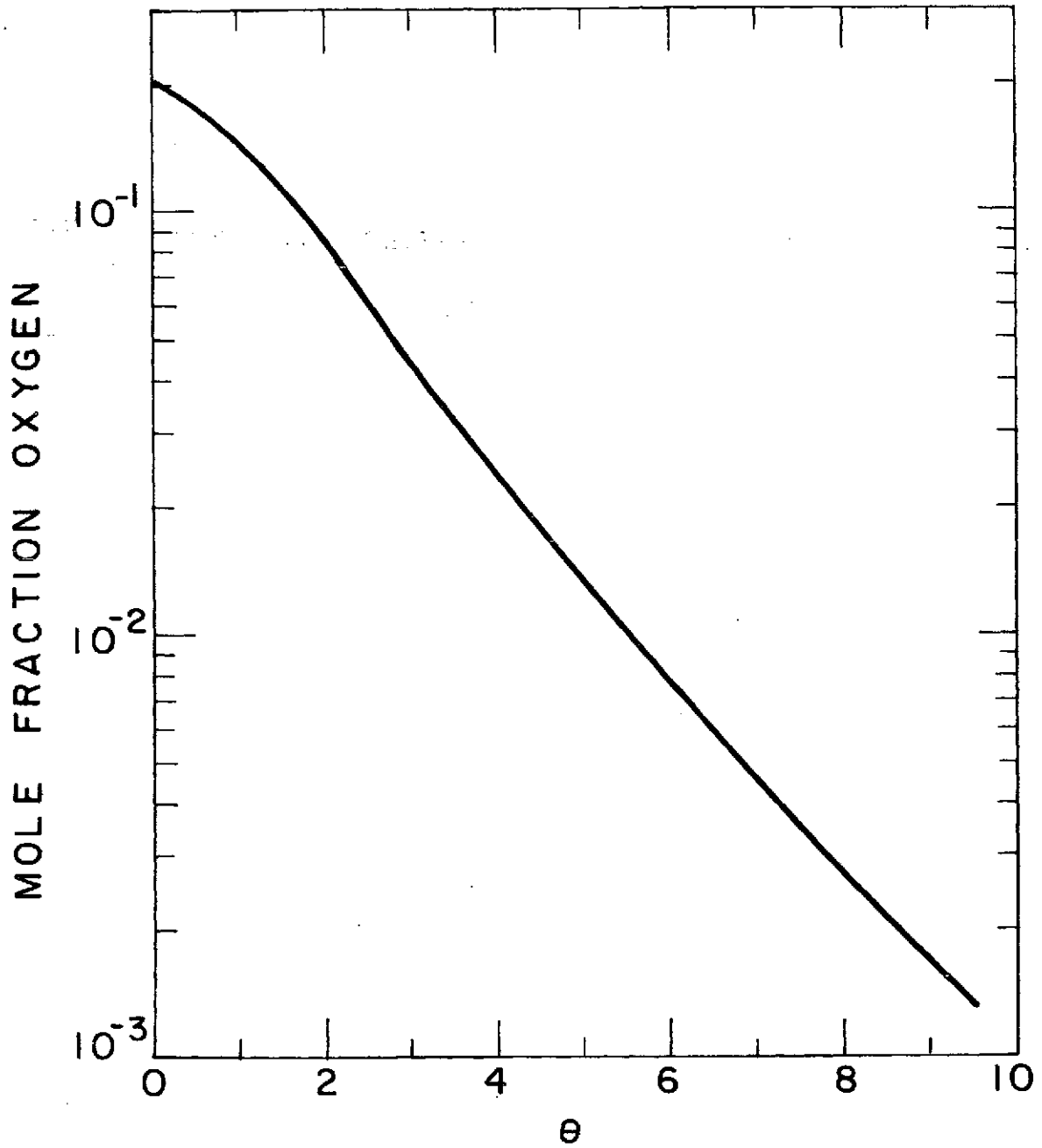


FIGURE 6

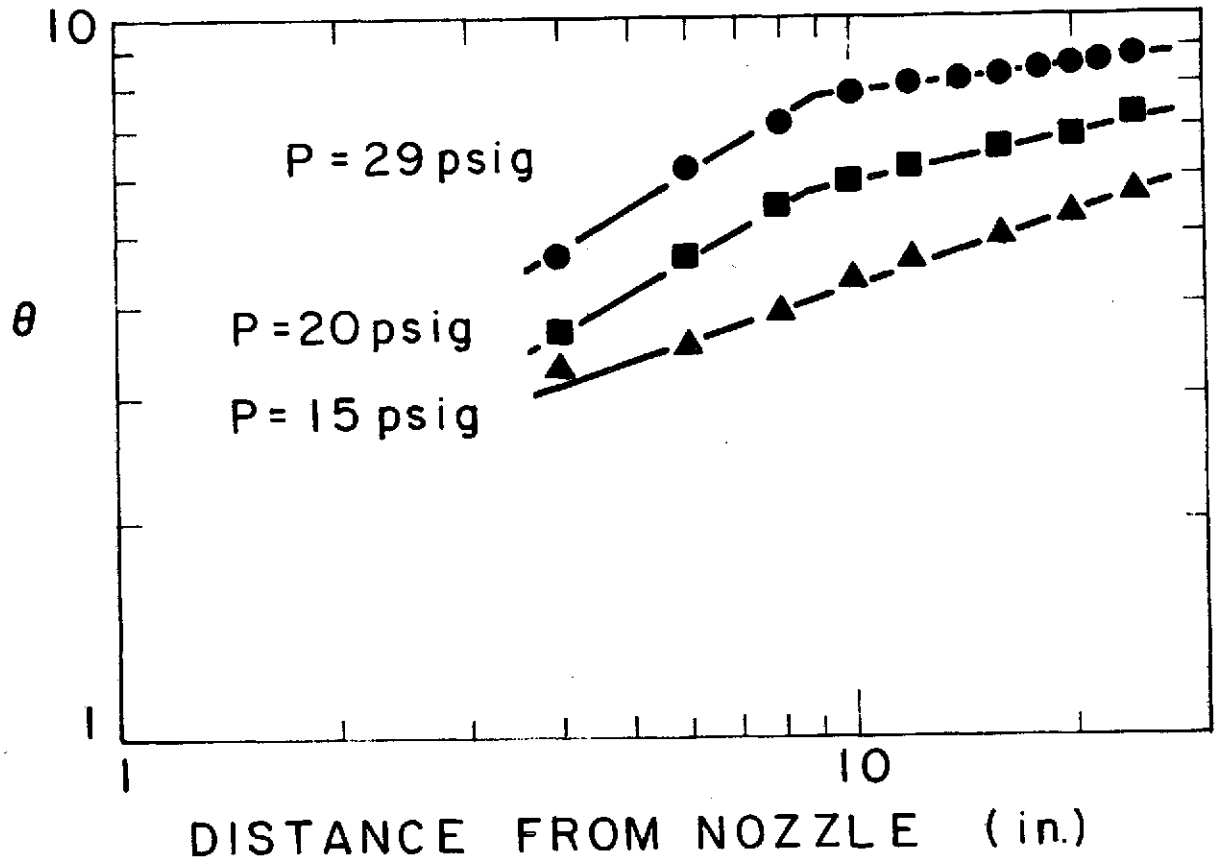


FIGURE 7

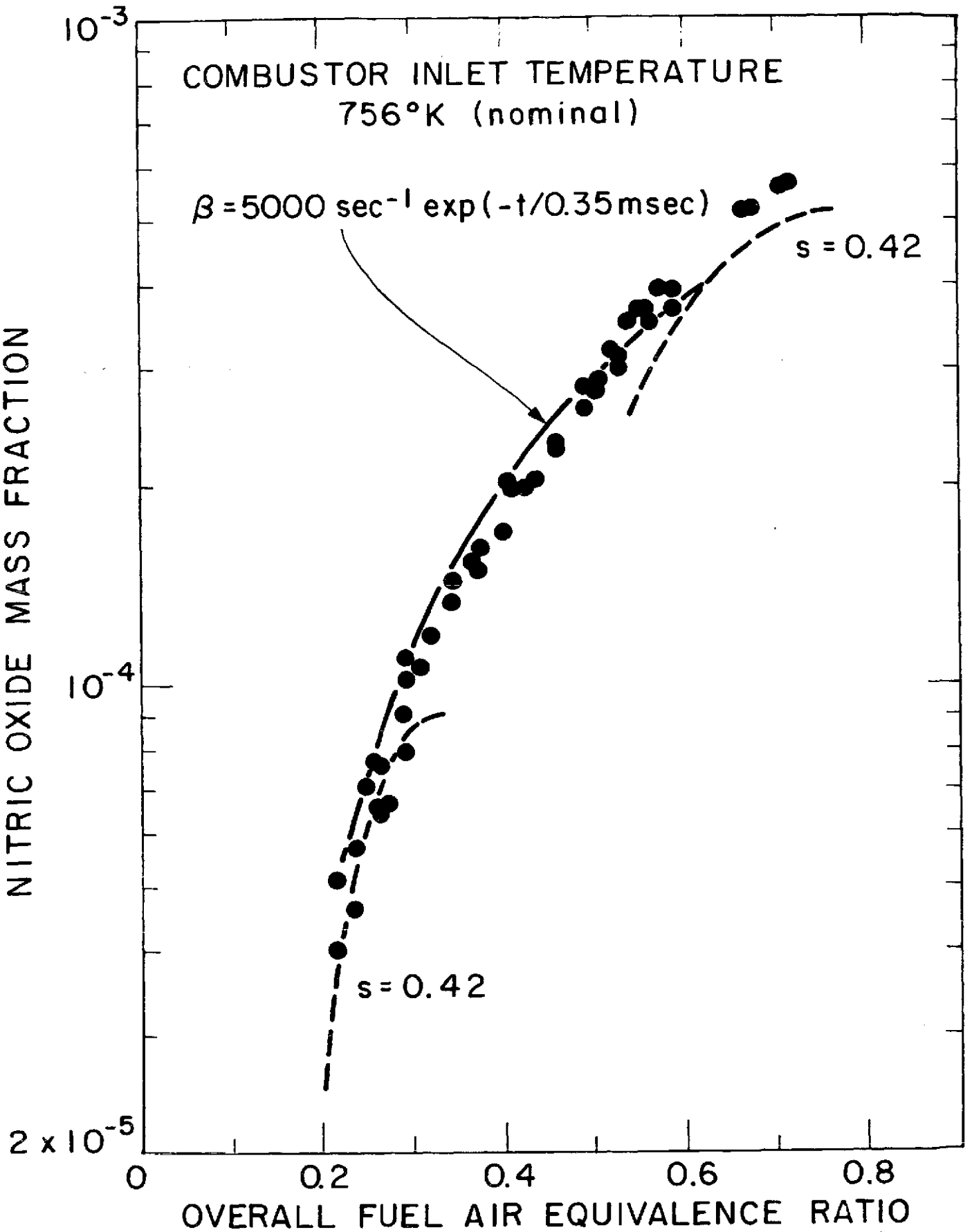


FIGURE 8



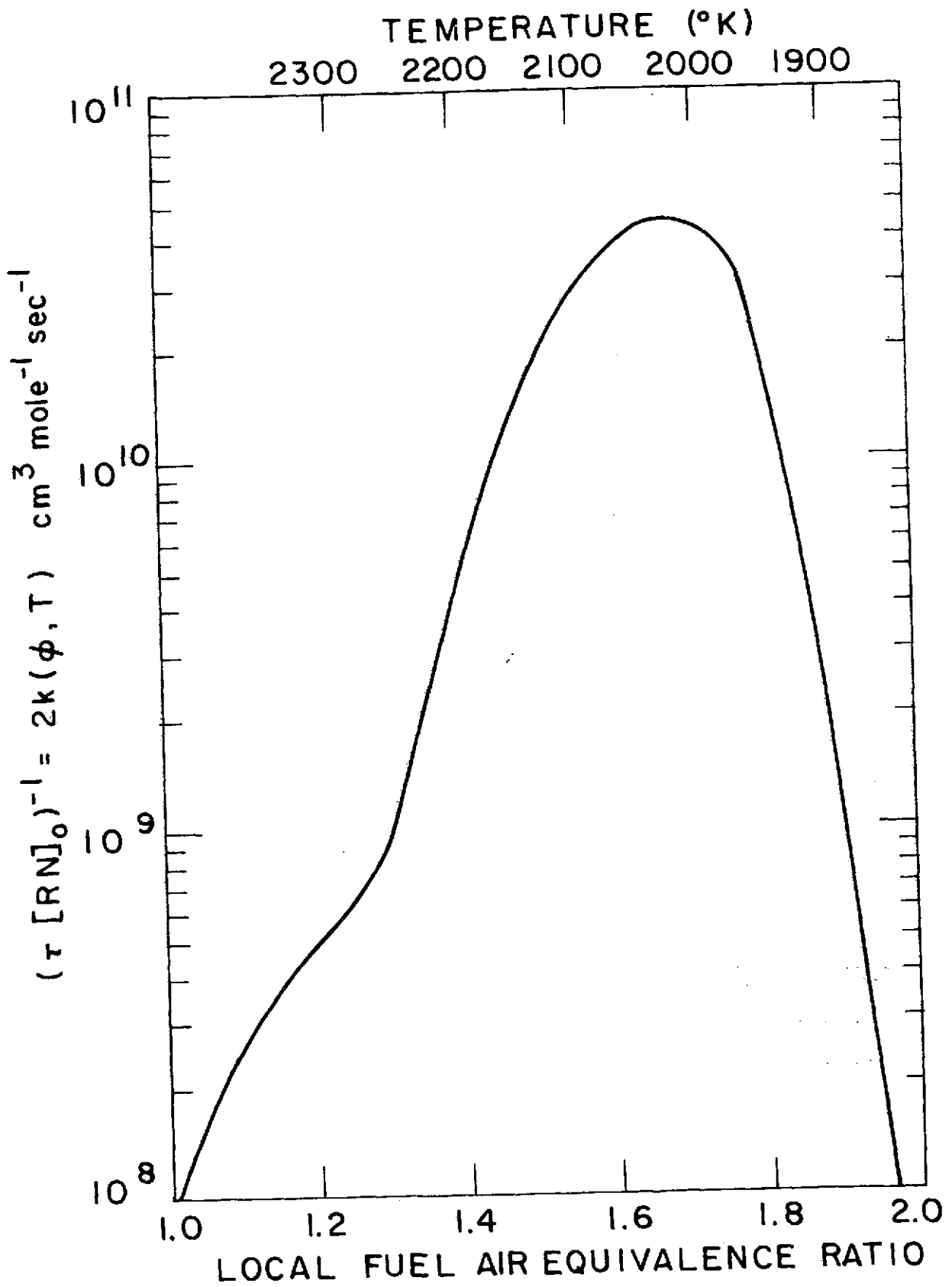


FIGURE 9

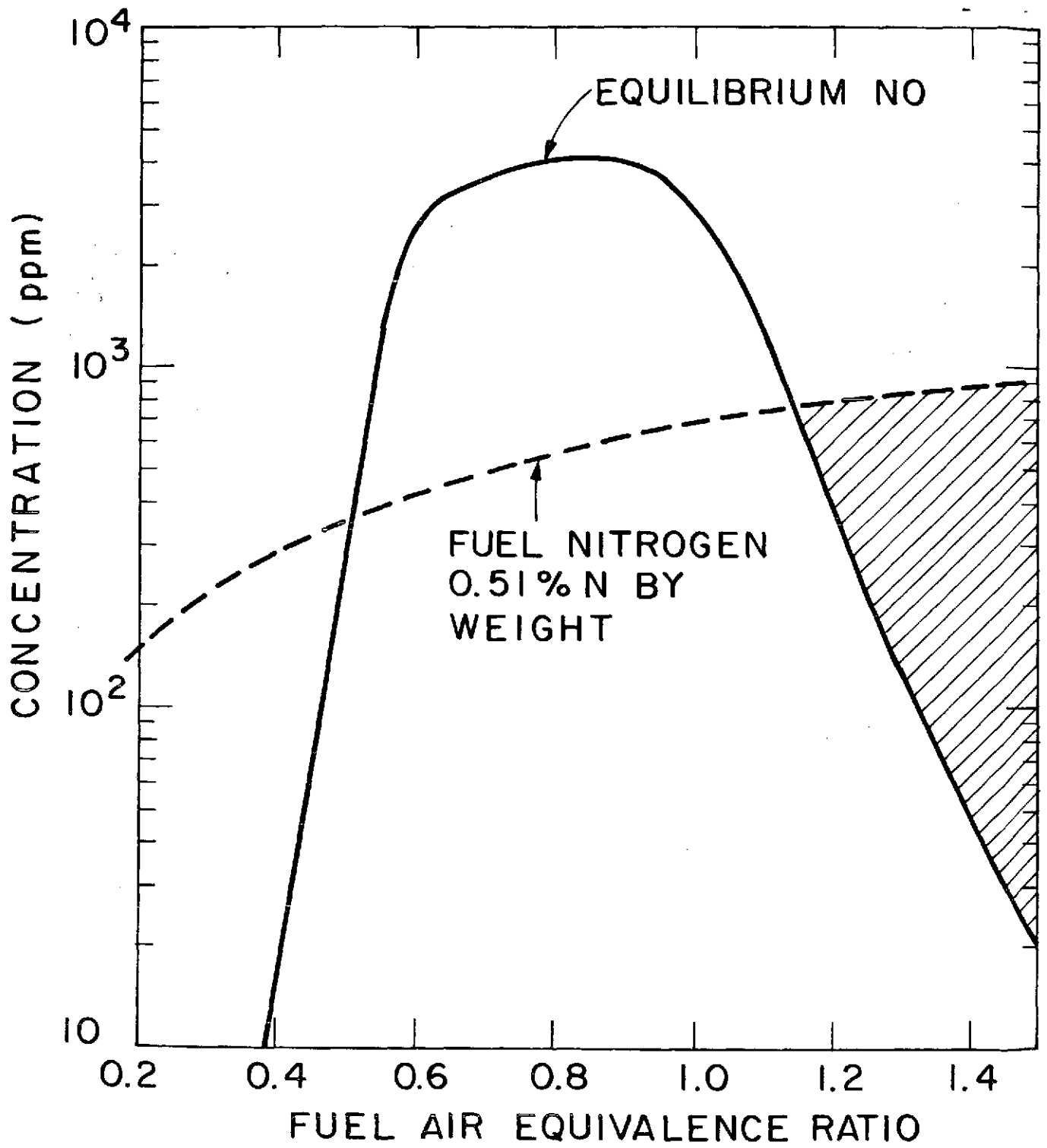


FIGURE 10

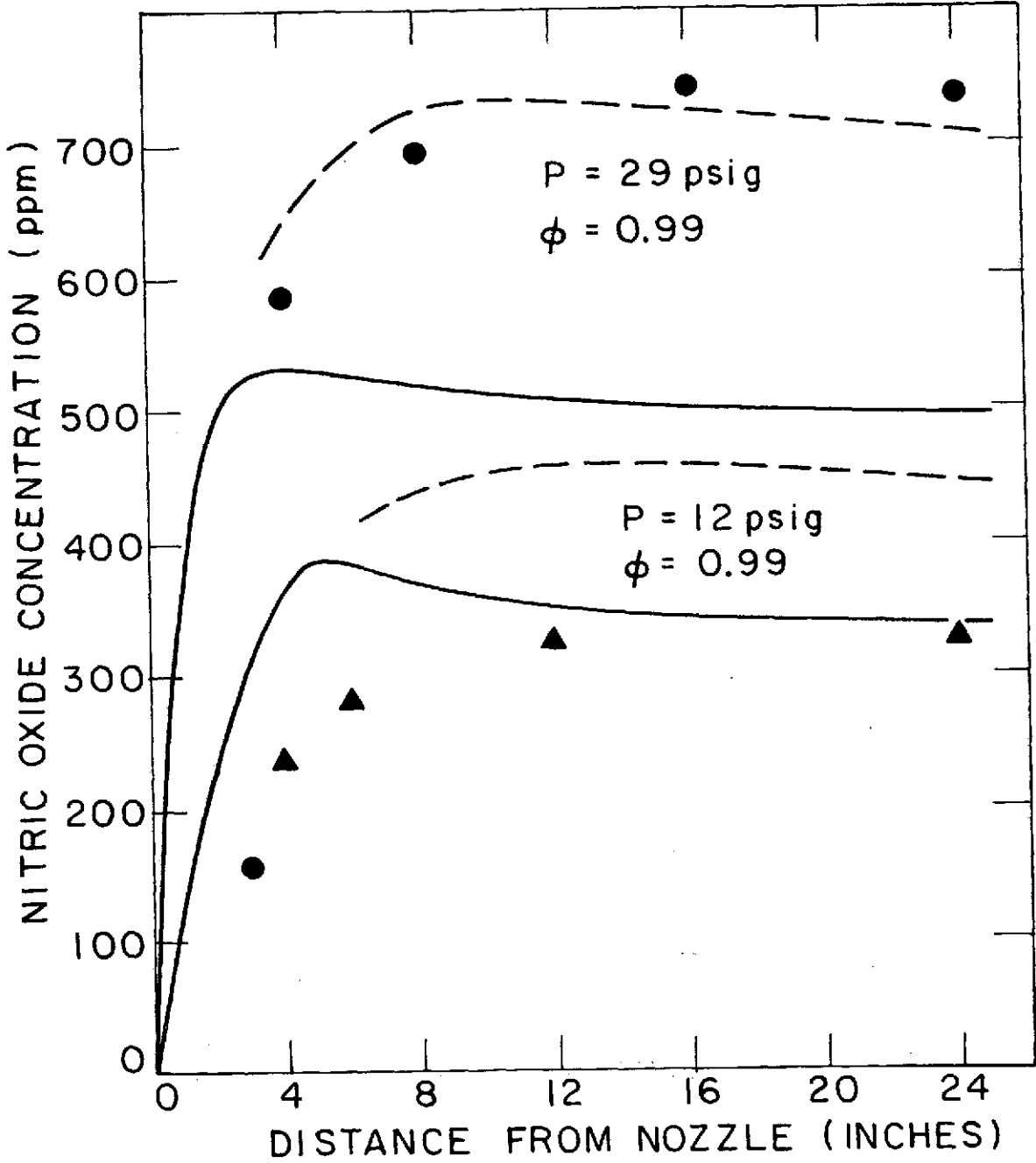


FIGURE II

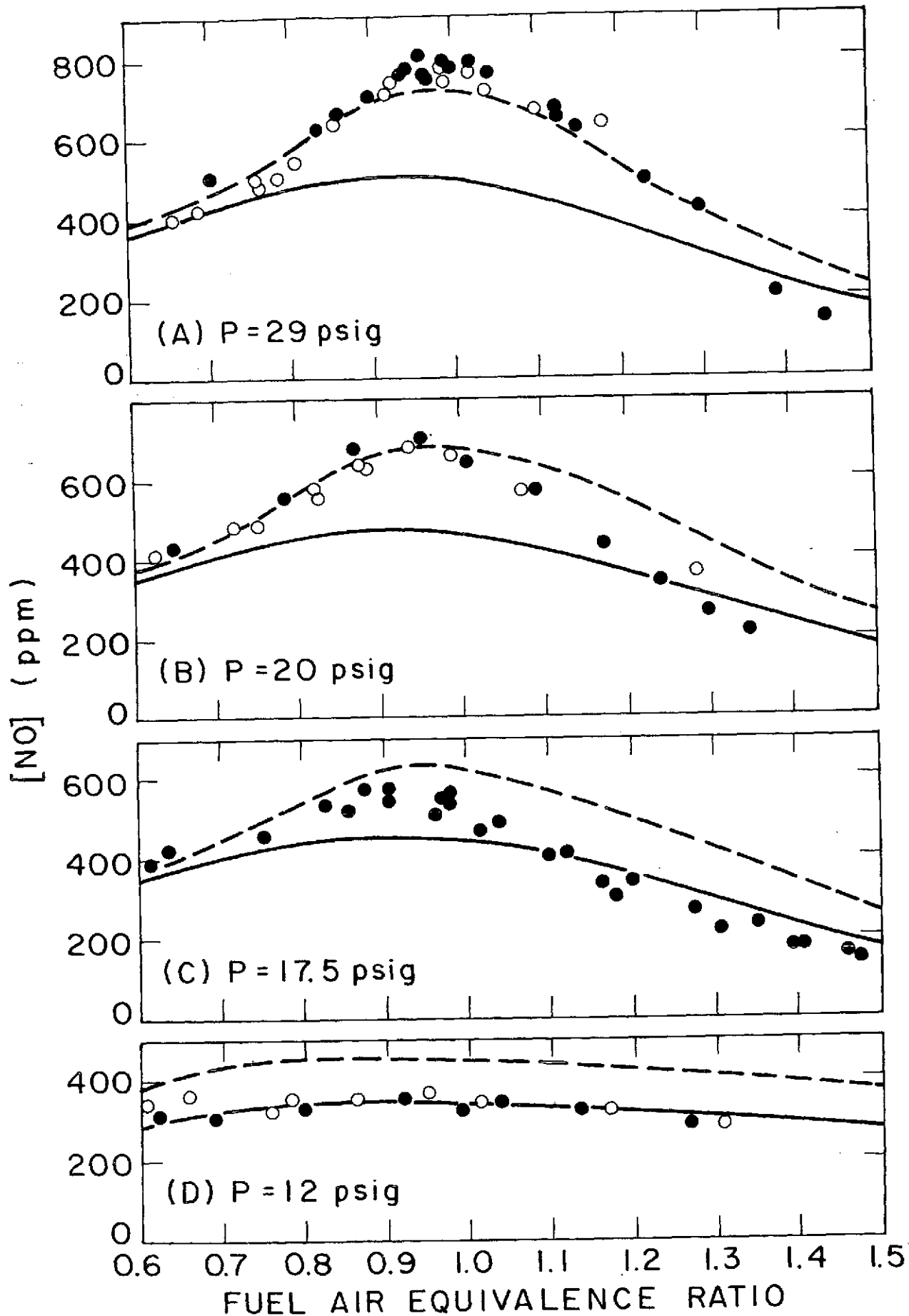


FIGURE 12

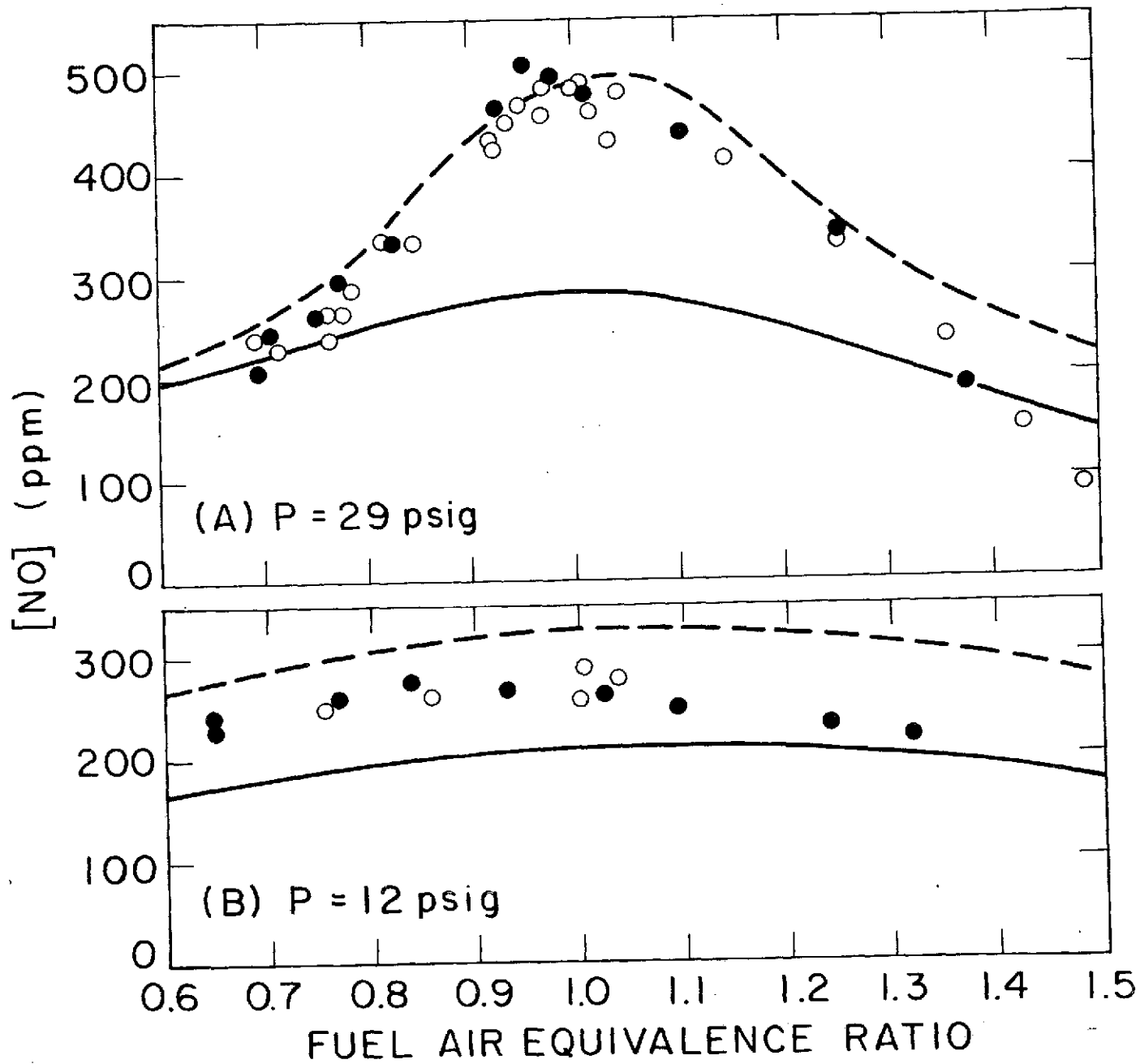


FIGURE 13

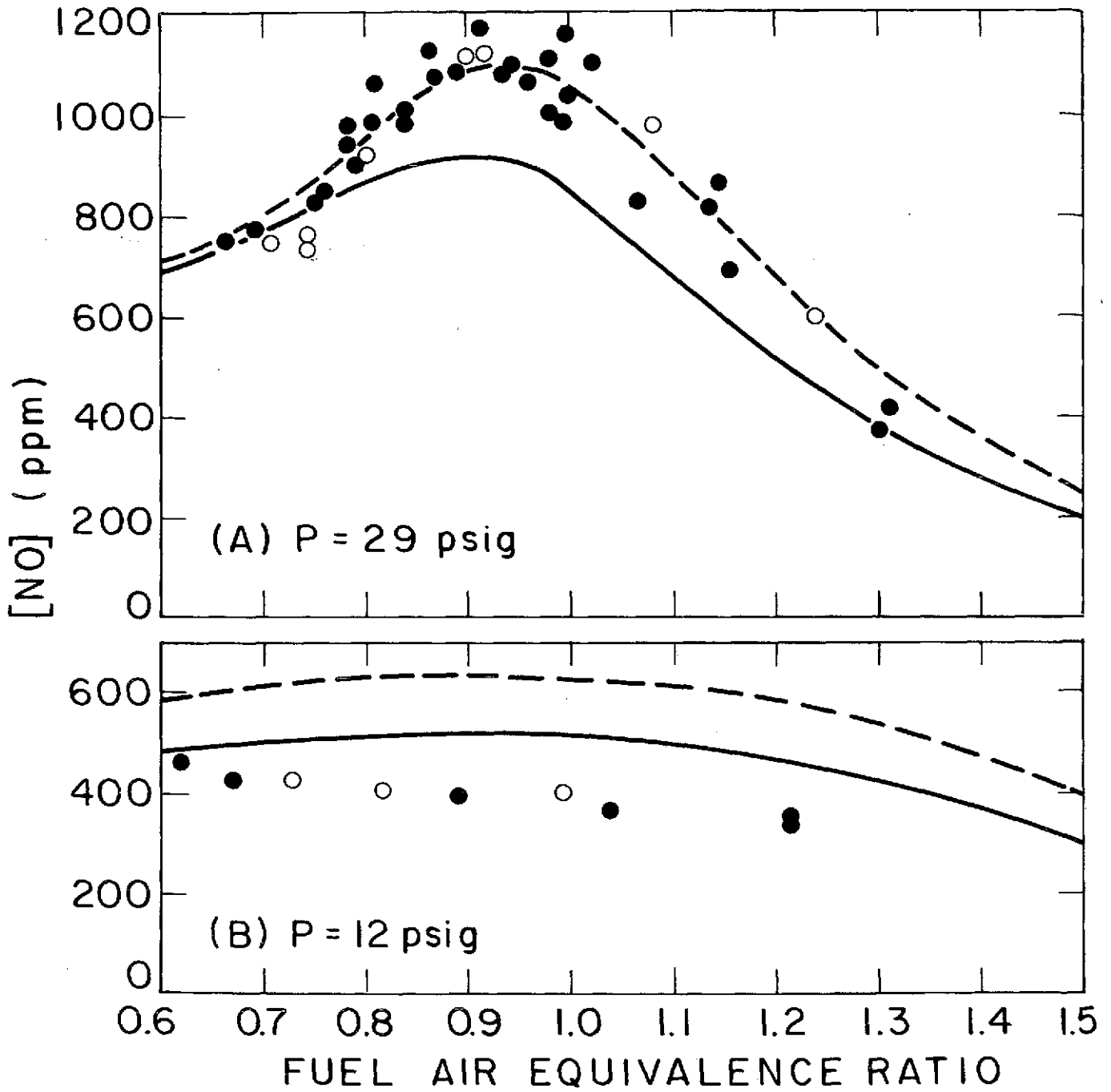


FIGURE 14

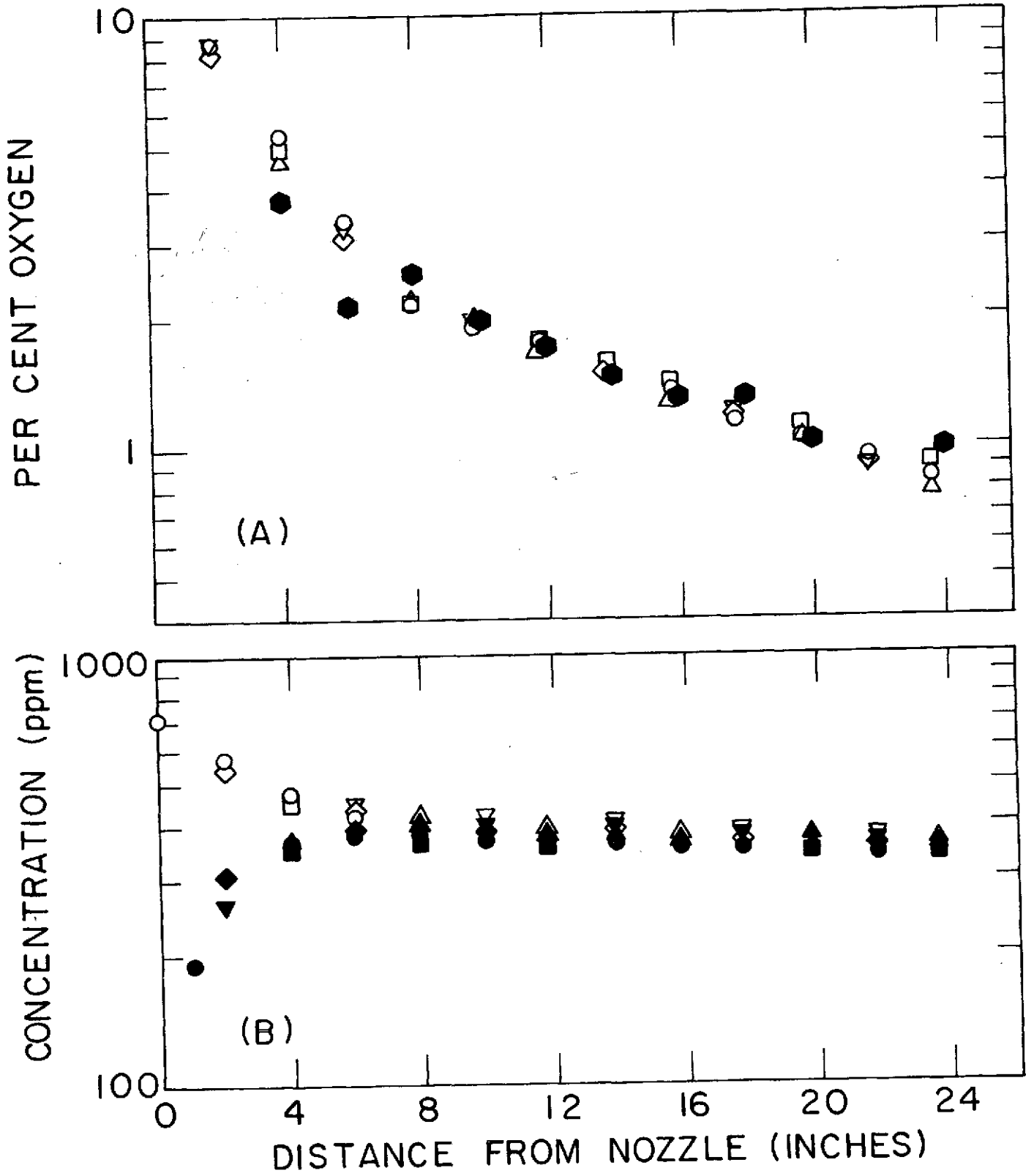


FIGURE 15